SRNL-STI-2011-00244

Key Words:
Mixing, CFD, Solid Suspension

Retention:
Permanent

TANK48 CFD MODELING ANALYSIS

APRIL 2011

Savannah River National Laboratory
Savannah River Nuclear Solutions
Aiken, SC 29808

Prepared for the U.S. Department of Energy Under Contract Number DE-AC09-08SR22470

SRNL

DISCLAIMER

Printed in the United States of America

Prepared for
U.S. Department of Energy

SRNL-STI-2011-00244

Key Words:
Mixing, CFD, Solid Suspension

Retention:
Permanent

TANK48 CFD MODELING ANALYSIS

Si Y. Lee
Sinjae Hyun*
***Professor, Mercer University, Macon, GA**

APRIL 2011

Savannah River National Laboratory
Savannah River Nuclear Solutions
Savannah River Site
Aiken, SC 29808

Prepared for the U.S. Department of Energy Under
Contract Number DE-AC09-08SR22470

TABLE OF CONTENTS

LIST OF FIGURES

LIST OF TABLES

NOMENCLATURE

A	Area
A_p	Projected cross-sectional area
c	volume fraction
C_D	Drag coefficient
C_o	Constant used in Eq. (1)
D	Tank diameter
d_o	Jet nozzle diameter
d_p	Particle diameter
E	Kinetic energy
f_1	Empirical function
f_2	Empirical function
g	Gravitational acceleration
h_o	Jet elevation height
K	Constant used in Eq. (1)
L	Jet length or maximum integral length scale
M	Fluid momentum
p	Pressure
Δp	Pressure drop
Q	Volumetric flow rate
Q_j	Jet volumetric flow rate
R	Tank or pipe radius
t	Time
U_o	Velocity at jet nozzle exit
U	Local velocity along the jet discharge direction
u	Local velocity along the x-axis
v	Local velocity along the y-axis
V_f	Fluid velocity
V_r	Relative settling velocity
w	Local velocity along the z-axis
W	Weight fraction
vol%	Volume percentage
wt%	Weight percentage
v(x)	Local velocity at a point x
x	Local distance along the x-axis
y	Local distance along the y-axis
z	Local distance along the z-axis
ρ_f	Fluid density
ρ_s	Solid density
ν	Kinematic viscosity
μ	Dynamic viscosity
η	Ratio of jet discharge distance to jet diameter
θ	Jet pump orientation angle
φ	Ratio of particle volume to the projected area
φ_v	Non-dimensional velocity distribution
gpm	Gallons per minute
inch	1 inch = 0.0254 m

Re	Reynolds number
Re_{jet}	Reynolds number based on jet operating conditions
CFD	Computational Fluid Dynamics
CFX	CFD software code
DOE	United States Department of Energy
ECR	Effective Cleaning Radius
FBSR	Fluidized Bed Steam Reformer
FLUENT	CFD software code
SRS	Savannah River Site
SWPF	Salt Waste Processing Facility

1.0 ABSTRACT

The process of recovering the waste in storage tanks at the Savannah River Site (SRS) typically requires mixing the contents of the tank to ensure uniformity of the discharge stream. Mixing is accomplished with one to four dual-nozzle slurry pumps located within the tank liquid. For the work, a Tank 48 simulation model with a maximum of four slurry pumps in operation has been developed to estimate flow patterns for efficient solid mixing. The modeling calculations were performed by using two modeling approaches. One approach is a single-phase Computational Fluid Dynamics (CFD) model to evaluate the flow patterns and qualitative mixing behaviors for a range of different modeling conditions since the model was previously benchmarked against the test results. The other is a two-phase CFD model to estimate solid concentrations in a quantitative way by solving the Eulerian governing equations for the continuous fluid and discrete solid phases over the entire fluid domain of Tank 48. The two-phase results should be considered as the preliminary scoping calculations since the model was not validated against the test results yet.

A series of sensitivity calculations for different numbers of pumps and operating conditions has been performed to provide operational guidance for solids suspension and mixing in the tank. In the analysis, the pump was assumed to be stationary. Major solid obstructions including the pump housing, the pump columns, and the 82 inch central support column were included. The steady state and three-dimensional analyses with a two-equation turbulence model were performed with FLUENT™ for the single-phase approach and CFX for the two-phase approach. Recommended operational guidance was developed assuming that local fluid velocity can be used as a measure of sludge suspension and spatial mixing under single-phase tank model. For quantitative analysis, a two-phase fluid-solid model was developed for the same modeling conditions as the single-phase model.

The modeling results show that the flow patterns driven by four pump operation satisfy the solid suspension requirement, and the average solid concentration at the plane of the transfer pump inlet is about 12% higher than the tank average concentrations for the 70 inch tank level and about the same as the tank average value for the 29 inch liquid level. When one of the four pumps is not operated, the flow patterns are satisfied with the minimum suspension velocity criterion. However, the solid concentration near the tank bottom is increased by about 30%, although the average solid concentrations near the transfer pump inlet have about the same value as the four-pump baseline results. The flow pattern results show that although the two-pump case satisfies the minimum velocity requirement to suspend the sludge particles, it provides the marginal mixing results for the heavier or larger insoluble materials such as MST and KTPB particles.

The results demonstrated that when more than one jet are aiming at the same position of the mixing tank domain, inefficient flow patterns are provided due to the highly localized momentum dissipation, resulting in inactive suspension zone. Thus, after completion of the indexed solids suspension, pump rotations are recommended to avoid producing the non-uniform flow patterns. It is noted that when tank liquid level is reduced from the highest level of 70 inches to the minimum level of 29 inches for a given number of operating pumps, the solid mixing efficiency becomes better since the ratio of the pump power to the mixing volume becomes larger. These results are consistent with the literature results [Tatterson, 1991].

2.0 INTRODUCTION

The process of recovering the waste in storage tanks at the Savannah River Site (SRS) typically requires mixing the contents of the tank to ensure uniformity of the discharge stream [Jacobs, 2010]. Mixing is accomplished with one to four slurry pumps located within the tank liquid. The slurry pump may be fixed in position or they may rotate depending on the specific mixing requirements.

The high-level waste in Tank 48 contains insoluble solids in the form of tetraphenyl borate compounds and monosodium titanate. Tank 48 is equipped with 4 slurry pumps, which are intended to suspend the insoluble solids prior to transfer of the waste to the Fluidized Bed Steam Reformer (FBSR) process. The FBSR process is being designed for a normal feed of 3.05 wt% insoluble solids, but will be capable of handling a high solids feed of 10 wt% insoluble solids. A chemical characterization study has shown the insoluble solids concentration is approximately 3.05 wt% when well-mixed. The project is requesting a Computational Fluid Dynamics (CFD) mixing study from SRNL to determine the solids behavior with 2, 3, and 4 slurry pumps in operation and an estimate of the insoluble solids concentration at the suction of the transfer pump to the FBSR process. The impact of cooling coils is not considered in the current initial work, but it will be added to the analysis as time and funding allow as the 2nd phase of work. The primary reason to neglect the presence of the cooling coils is that the results of this study will be used as an initial scoping phase to develop the operational strategy for the Tank 48 FBSR process. All of the solids accumulation and weight fraction information is expected to be approximate. An analytical data validation package is not included in this task scope.

The work consists of two principal objectives by taking a CFD approach:

- To estimate insoluble solids concentration transferred from Tank 48 to the Waste Feed Tank in the FBSR process and
- To assess the impact of different combinations of four slurry pumps on insoluble solids suspension and mixing in Tank 48.

For this work, several different combinations of a maximum of four pumps are considered to determine the resulting flow patterns and local flow velocities which are thought to be associated with sludge particle mixing. Two different elevations of pump nozzles are used for an assessment of the flow patterns on the tank mixing. Pump design and operating parameters used for the analysis are summarized in Table 1. The baseline pump orientations are chosen by the previous work [Lee and Dimenna, 2008] and the initial engineering judgement for the conservative flow estimate since the modeling results for the other pump orientations are compared with the baseline results. As shown in Table 1, the present study assumes that each slurry pump has 900 gpm flowrate for the tank mixing analysis, although the Standard Operating Procedure for Tank 48 currently limits the actual pump speed and flowrate to a value less than 900 gpm for a 29 inch liquid level. Table 2 shows material properties and weight distributions for the solids to be modeled for the mixing analysis in Tank 48.

Computational Fluid Dynamics (CFD) approach is taken by using the three-dimensional prototypic configuration of SRS Type-IIIA tank, Tank 48, as shown in Fig. 1. As shown in the figure, major solid obstructions including the tank wall, the pump housings, the transfer pump column, and the 82 inch central support column will be included in the flow

performance model. Flow obstructions due to the presence of the cooling coils are assumed to be negligible for the initial scoping calculations.

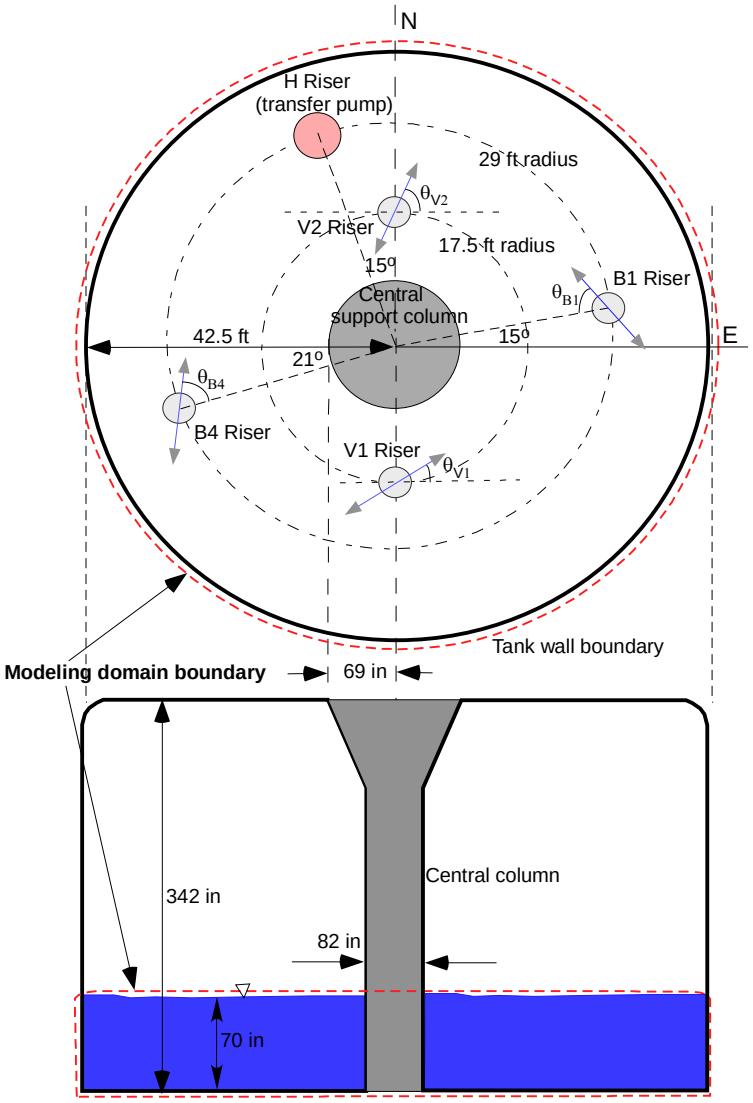

Figure 1. Geometrical configurations and three-dimensional modeling domain containing four slurry pumps and one transfer pump in the analysis of the Tank 48 performance model

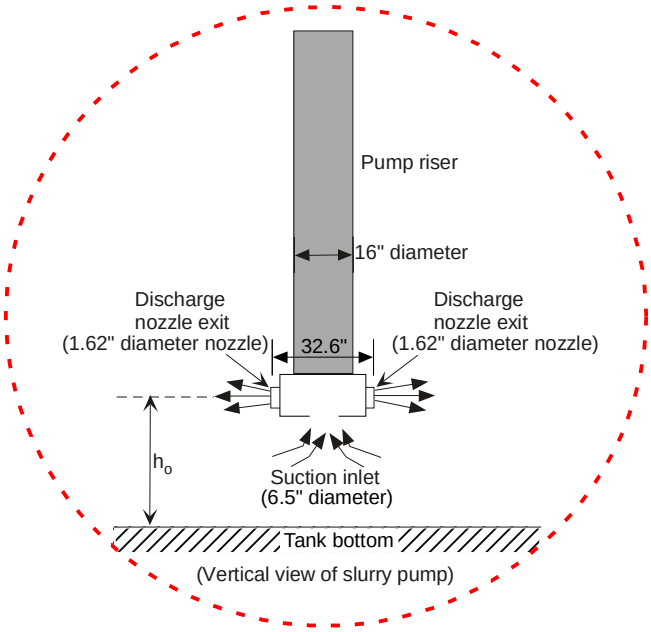

Figure 2. Geometrical configurations for one of the four slurry pumps located at B1, B4, V1, and V2 risers in the modeling analysis

Table 1. Pump design parameters for slurry pump used for the baseline analysis

Pumps	**Slurry pump**
Number of nozzles	2
Flow rate per nozzle, gpm	900 (2 nozzles)
Number of pumps	Up to 4
Nozzle diameter, d_o, inches	1.62”
Pump rotation (for the present analysis)	No (Indexed pump)
Pump nozzle elevation above tank bottom (h_o in Fig. 2), inches	16.81” for B1 and B4 pumps, 19.81” for V1 and V2 pumps
Pump nozzle directions (angles indicated in Fig. 1)	$\theta_{B1}=45^o$, $\theta_{B4}=45^o$, $\theta_{V1}=22.5^o$, $\theta_{V2}=67.5^o$
Tank liquid level, inches	70, 29*
Velocity at nozzle exit, U_o, ft/sec (m/sec)	70.04 (21.35)
Pump $U_o d_o$, ft^2/sec	9.46

Note:*Minimum tank liquid level for sensitivity analysis

Table 2. Material properties and weight distributions for the solids contained in Tank 48

Solids material	Size range++ (microns)	Nominal size for modeling (microns)	Density (gm/cm^3)	Weight distributions+ (wt%)
MST	4 - 5	5	1.80	0.15
			2.765*	0.15
KTPB	≤ 40	40	1.18	2.01
Sludge	2 - 16	16	1.20**	0.89

Note:+[Thomas, 2006]
++[Baughman, 2010]
*Used for the modeling analysis for conservative estimate [Hobbs, 2007]
**[Poirier, 2011, and WSRC-TR-97-0360]

3.0 SOLUTION APPROACH AND FLOW CRITERIA

A three-dimensional CFD approach is used to calculate flow patterns for the sludge mixing operations of Tank 48 and to evaluate sludge suspension capabilities for the tank. The work used two different solution methods for the modeling analysis. One is a single-phase CFD approach by using the previous method with FLUENT code [3,4] since the model predictions were in good agreement with test data and operational observations. The other is a two-phase approach of fluid and solid phases by CFX code to quantify the solid concentrations near the transfer pump. For the modeling calculations, a prototypic geometry is modeled by hexahedral and tetrahedral meshes over the computational domain. The modeling domain to be used for the present analysis is presented in Fig. 1. Nominal design and operating conditions of the pumps used in the Tank 48 model are presented in Table 1.

Based on the modeling domain and operating conditions, turbulent flow calculations were performed. Typical flow conditions for the slurry pump corresponds to fully-developed turbulent flow since Reynolds numbers are about $1x10^6$ in terms of pump discharge conditions. For the turbulence calculations, the standard k–ε model was used. The three-dimensional model was run in steady state mode for the indexed pump conditions to establish the jet flow patterns. For the single-phase approach, local fluid velocity at any distance from the nozzle is employed as a measure of the slurrying and mixing effectiveness in Tank 48H operations.

The present work focuses on suspending and mixing sludge particles with the turbulent jet generated by a combination of up to four slurry pumps in Tank 48. Prior to discussing the computational modeling assumptions, some literature results for a free turbulent jet flow are reviewed briefly, since the free jet flow is similar in many respects to the bounded wall jet. The previous work [Lee et al., 2008] and the literature data [Abramovich, 1963] show that when a turbulent jet of fluid is discharged from a nozzle with a diameter d_o, it both entrains fluid and expands. Most mixing action and entrainment takes place in the region of fully-developed flow which begins at a distance of approximately eight nozzle diameters from the exit plane. The non-dimensional velocity distribution φ_v along the jet axis of this region for a homogeneous fluid jet is given by [Lee et al., 2008] as

$$\varphi_v = \left(\frac{v(x)}{U_o} \right) = C_o \left[\frac{x}{d_o} \right]^{-1} = C_o \, \eta^{-1} \qquad (1)$$

In Eq. (1), C_o is a constant determined by the turbulence characteristics of the jet, U_o, the average velocity at nozzle exit, $v(x)$, the local velocity at a point *x*, and *x* , the distance from nozzle. For a free jet without any flow obstructions, the proportionality constant C_o in Eq. (1) was determined to be 6.32 [Abramovich, 1963]. Since the pump discharge flow inside large-scale tanks at SRS is affected by the bottom of the tank and internal flow recirculation, C_o is replaced by a constant *K* evaluated from the previous Tank 18 calculations, rather than classical free jet theory. *K* was found to be 4.874 [Lee and Dimenna, 2001]. Typical velocity profiles in the direction perpendicular to the free surface from the previous modeling results of large-scale tank mixing simulations are shown in Fig. 3. The maximum axial velocity at any axial position *x* can be estimated using Eq. (1). The equation shows that the velocity at any point in the region of established flow is directly proportional to the product, $d_o U_o$. Thus, the axial entraining distance corresponding to minimum entrainment velocity can be estimated with nozzle diameter and flow rate.

The fluid domain for Tank 48 has both a solid wall boundary and a free surface boundary as the jet expands into the downstream region and ultimately recirculates via the suction on the bottom of the pump as shown in Fig. 1. The spreading fluid is retarded by the interaction with the wall, and the inner part of the flow may be expected to show a certain structural similarity to a boundary layer. Entrainment of quiescent fluid occurs near the outer edges of the flow, and accordingly resembles a free jet [Abramovich, 1963]. In this case, sludge particles settled near the edge of the boundary region are entrained into a turbulent zone, and they are suspended. Estimations of minimum suspension velocity and particle settling rate will be discussed for establishment of a flow velocity criterion in the subsequent sections.

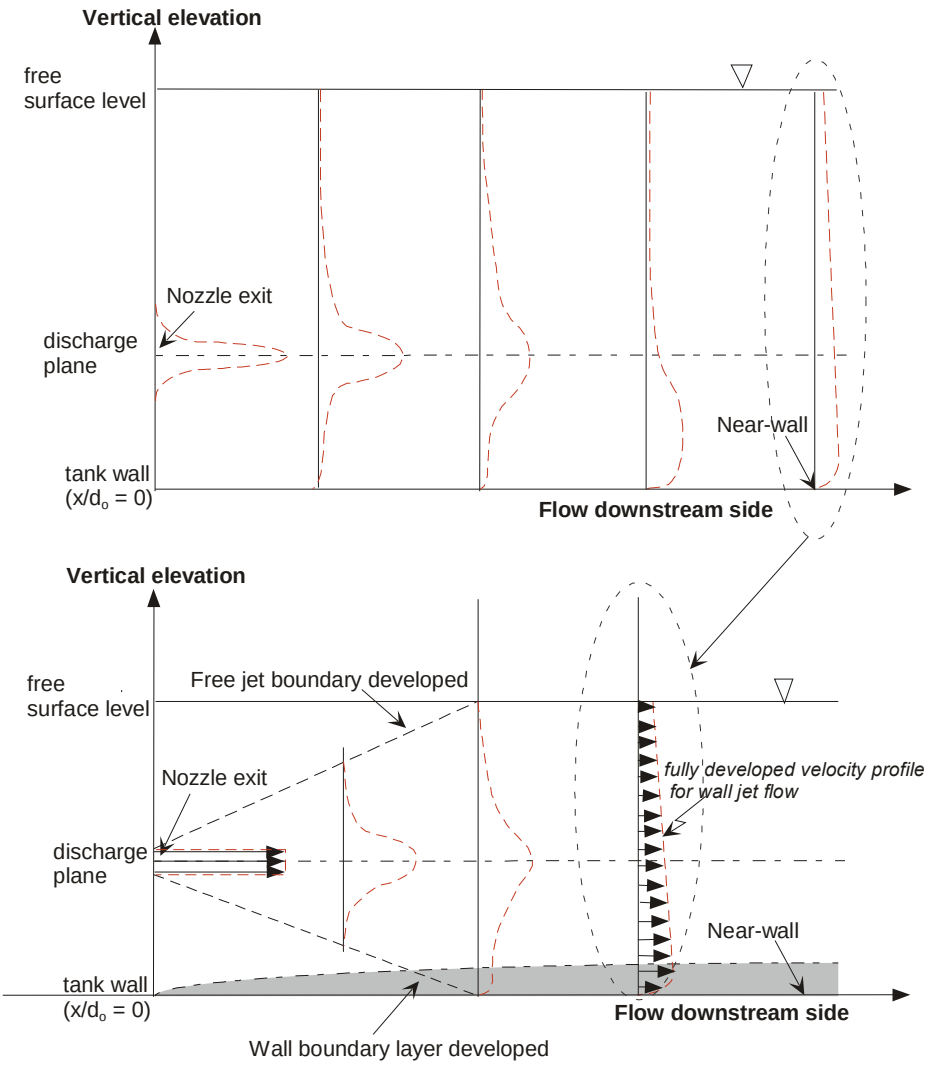

Figure 3. Typical velocity profiles in the direction perpendicular to the free surface from the previous modeling results of large-scale tank mixing simulations [Lee et al, 2008].

3.1 ESTIMATION OF MINIMUM SUSPENSION VELOCITY DURING JET MIXING

The decay of the axial jet velocity and the evolution of flow patterns are important phenomena affecting sludge suspension and mixing operations. A measure of the ability to shear the solids layer, the scouring wall shear, is directly related to the local fluid velocity. The initial movement of solids deposited on the bottom of the tank identifies the critical condition or initial scour. It is usually described by two criteria, the minimum flow velocity and the frictional shear to scour and initiate movement of deposited solids particles. From these two criteria, a local fluid velocity can be determined as a performance indicator for adequate suspension.

When liquid flow passes over a settled solids layer containing small solids of 1 to 50 microns, the range of the sludge particles in Tank 48H, it results in hydrodynamic forces

being exerted on individual particles in the layer. For a particular stationary solids layer, a condition is eventually reached in which particles in the movable bed are not able to resist the hydrodynamic forces and solids in the top layer start to lift. Average flow velocity, particle size and density, and slurry flow regime are key parameters in determining the transport patterns of particles in a slurry [Lee et al., 2008]. The critical velocity is defined as the minimum velocity that can initiate the movement of the solids deposited near the bottom of the tank. Following the previous works [Lee et al., 2008], a literature correlation [Graf, 1971] for the critical velocity V_c was used.

$$V_c = \left(\frac{d}{H}\right)^{-0.1} \sqrt{2.5gd\left(\frac{\rho_s}{\rho_f} - 1\right)} \qquad (2)$$

In Eq. (2), d and H are the particle diameter and tank liquid level, respectively. ρ_s and ρ_f are solid and fluid densities, respectively. When the flow velocity required for sludge transport and suspension is exceeded, the solid-laden flow can be treated as a suspended fluid-solid mixture. In this case, although solid particles are suspended by the continuous-phase flow, the local amount of solids suspended by the fluid may not be uniform over the entire domain of the tank fluid. However, the present work assumes that when the flow velocity required for sludge transport and suspension is exceeded and transient turbulent kinetic energy is dissipated throughout the tank in a quasi-steady condition, the solid-laden flow can be approximated as a homogeneous fluid. Thus, a flow velocity required for sludge suspension will be used as criteria for particle suspension from different pump combinations and operations in Tank 48.

Table 3 presents nominal solids size and material properties for three different particulates contained in Tank 48. As shown in the table, MST particulate requires the largest velocity required to be suspended from the tank floor. Figure 4 shows minimum suspension velocities for particles of different mono-sized particle systems with different particle specific gravities (spg) with a tank level of 70 inches. Thus, local fluid velocity at any distance from the nozzle is employed as a measure of the slurrying and mixing criterion.

Table 3. Material properties and minimum suspension velocities for solids in Tank 48

Solids material	Nominal size (microns)	Density (gm/cm^3)	Tank liquid level (inches)	Suspension velocity (m/sec) [ft/sec]
MST	5	1.8	70	(0.036) [0.117]
		2.765	70	(0.053) [0.173]
KTPB	40	1.18	70	(0.039) [0.127]
Sludge	16	1.2	70	(0.028) [0.093]

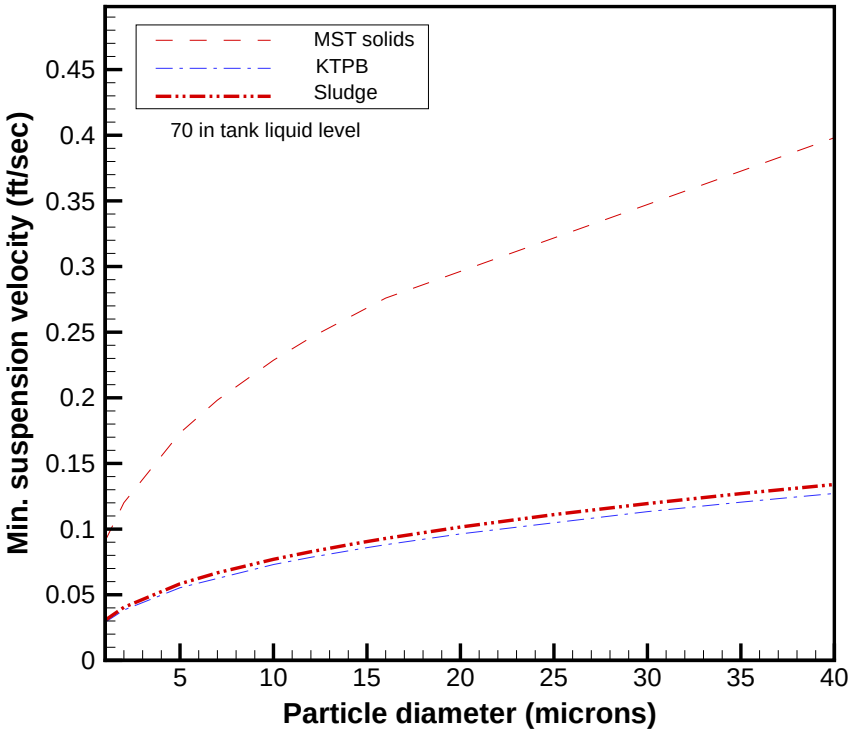

Figure 4. Minimum velocity required to suspend particle from the floor

3.2 SETTLING VELOCITY FOR MONO-SIZED PARTICLES IN STAGNANT FLUID

The drag force on an isolated solid particle moving in an infinite expanse stagnant fluid is represented by the equation,

$$F_D = \frac{1}{2} C_D \rho_f v_f^2 A_p \qquad (3)$$

In Eq. (3) ρ_f is density of fluid, A_p represents the projected cross-sectional area of the particle perpendicular to the direction of motion, and C_D is the drag coefficient at the surface of particle when a solid particle is falling downward with velocity v_f. The drag coefficient C_D is dependent on particle shape and flow regime in terms of the Reynolds number (*Re*).

For the case of free settling of spherical particles of density ρ_p at a constant velocity and without interaction or hindering effects due to the presence of other particles, the drag force F_D equals the force of gravity F_G, including the buoyancy force of the particle of solid volume V_p submerged in a quiescent fluid.

$$F_G = V_p (\rho_p - \rho_f) g$$
$$= F_D \qquad (4)$$

After some algebraic manipulations, eqs. (3) and (4) become

$$v_f = \left[\left(\frac{2}{C_D}\right)\left(\frac{V_p}{A_p}\right) g \frac{\left(\rho_p - \rho_f\right)}{\rho_f}\right]^{0.5} = \left[\left(\frac{2}{C_D}\right)\varphi g \frac{\left(\rho_p - \rho_f\right)}{\rho_f}\right]^{0.5} \quad (5)$$

When the particle has a spherical shape with diameter d_p, the ratio (φ) of the particle volume to its projected area in Eq. (5) is (2/3)d_p. Then,

$$v_f = \left[\left(\frac{4}{3C_D}\right) d_p g \frac{\left(\rho_p - \rho_f\right)}{\rho_f}\right]^{0.5} \quad (6)$$

In this situation, the flow is assumed to be slow viscous, or Stokes's flow. In 1850, Stokes derived the solution for viscous flow past a sphere at small values of the Reynolds number by using the momentum equation without inertia terms in a spherical polar coordinate system and by fitting no-slip boundary conditions at the spherical surface [9]. His result for drag force acting on the sphere was:

$$F_D = 3\pi\mu_f d_p U_o \quad (7)$$

where U_o is the undisturbed free stream velocity.

When the particle velocity relative to the bulk fluid is equal to the undisturbed free stream velocity in Eq. (7) and Re < 0.6, the drag coefficient C_D in Eq. (5) corresponding to the Stokes formula, Eq. (7), can be expressed as

$$C_D = \frac{F_D}{\frac{1}{8}\rho_f v_f{}^2 \left(\pi d_p{}^2\right)} = \frac{24}{Re} \quad (8)$$

The Reynolds number, *Re,* the dimensionless parameter used in Eq. (8), is defined in terms of particle diameter d_p and velocity v_f relative to the fluid medium with density ρ_f and viscosity μ_f as,

$$Re = \frac{d_p \rho_f v_f}{\mu_f} \quad (9)$$

When the drag coefficient C_D in Eq. (6) is replaced by Eq. (8), settling velocity for a single spherical particle in quiescent fluid becomes

$$v_f = \frac{g d_p{}^2 \left(\rho_p - \rho_f\right)}{18\mu_f} \quad (10)$$

It must be emphasized that Stokes's drag coefficient is only applicable at very low velocities and valid for values of Reynolds number less than about 1. This limit for Stokes flow corresponds to viscous dominant settling velocity.

At larger values of the Reynolds number, the inertial terms exercise an increasing influence on the flow dynamics. From the literature [13], the drag coefficients for the spherical particle submerged in the fluid are as follows:

$$C_D \approx \frac{18.5}{Re^{0.6}} \quad \text{for } 1 \le Re < 10^3 \text{ (intermediate flow regime)}$$

$$C_D \approx 0.44 \quad \text{for } 10^3 \le Re < 10^5 \text{ (Newton's flow regime)} \quad (11)$$

The study of settling phenomena has been performed by a considerable diversity of approaches. The literature information [11] has suggested that the motion of a typical single particle should be influenced by both the motion and the presence of the other particles. The main effect of the motion of the other particles is to cause a return flow of liquid, while the presence of the other particles produced an effect similar to an increase in the viscosity of the dispersing liquid. In the literature correlations [13], the velocity for flow past a single sphere was used in order to obtain an equation relating the settling velocity of a suspension of mono-size spherical particles to the volume concentration of the solid phase.

Table 3 shows a useful correlation for relative settling velocity V_r in terms of solids volume concentration, c. Relative settling velocity V_r is defined as

$$V_r = \frac{v_s}{v_f} \tag{12}$$

In Eq. (12), v_s is the settling velocity in a multi-particle system, and v_f is the settling velocity for a single particle in a fluid.

The downward motion of the particles must cause an upward flow of liquid, and the velocity of this flow averaged for the whole flow cross-section of the tank must be the liquid fraction (1 - c) times the solid settling velocity of particles, allowing only for return flow of liquid when c is defined as the solids volume fraction of the solid-fluid mixture. In addition, the presence of other particles also impedes the motion of a given particle in the same way as if there were an increase in the viscosity of the liquid, so that the effective relative viscosity would reduce the settling rate of the suspended particles. Thus, the updated literature correlations [11] for settling velocity within a solution containing low solids volume fraction were formulated considering these two factors.

$$v_s = v_f \, f_1(c) f_2(c) \tag{13}$$

In Eq. (13) f_1 and f_2 are empirical functions associated with a return flow effect due to the falling of the particles and a hindering effect of the particle precipitation due to the increased effective viscosity, respectively. These two functions were assumed to be dependent only on the solid volume fraction of suspension, c.

A typical literature correlation for relative settling velocity is shown in Table 4. It can be used to examine the interference or hindering effects of particle settling due to presence of the other particles for the range of solid particle concentrations. The results shown in the literature indicate that settling velocities of particles in a multi-particle system are different depending on the particle shape and solid concentration. The settling velocity of spherical particles was estimated for different solid contents in a slurry. The Oliver (1961) correlation was used to capture the hindering effect of particle settling in a multi-particle system. Specific information on the waste characteristics for the present work assumes that the insoluble solids have particle sizes from 5 to 40 microns with a concentration of about 3.1 wt%, a slurry solids density of 1200 to 2800 kg/m^3, and a fluid viscosity of 1 x 10^{-3} Pa-s for a conservative estimate of the sludge settling rate. The volume concentration of particles in the continuous fluid phase is one of the key parameters associated with flow pattern and slurry characteristics. The weight fraction W for solids can be converted to volume fraction c for given densities of the fluid and solid phases.

$$c = 1 - \left\{ \frac{\left(\frac{\rho_f}{\rho_s}\right)}{\left(\frac{1}{W} - 1\right)} + 1 \right\}^{-1} \tag{14}$$

where ρ_f and ρ_s are the densities of fluid and solid, respectively.

From Eq. (14) volume fractions of slurry solids (*c*) can be calculated as about 0.0246 for the present operating conditions when their weight fractions in a slurry flow are 0.0305. The results for settling velocity of the sludge particle are summarized in Table 5. It is noted that a 16-micron sludge particle takes longer than 2 hours to settle without hindering effects from the inlet of the transfer pump to the tank floor. Figure 5 shows single free-fall velocities and multi-particle settling velocities as function of solid particle diameters in tank fluid. The calculations were performed by using a Stokes's flow approach (Eq. (10)) and the literature correlation for the settling rate of mono-sized spherical particles. The results show that it takes a range of about 2 hours to one day for the largest particles, KTPB solid, in a stagnant tank fluid to be settled down to the tank floor. It is noted that when the tank fluid is in motion, the settling time will be longer than the 2 hours' stagnant settling time.

Table 4. Literature correlation for relative settling velocity based on solid volume fraction (relative settling velocity V_r is defined by Eq. (12)).

Authors (Year)	Relative settling velocity correlations	Approach method
Oliver (1961)	$V_r = \left(1 - 0.75c^{1/3}\right)(1 - 2.15c)$	Theoretical and empirical work

Table 5. Settling velocity and average settling times in slurries containing three different solid contents (ρ_f = 1.0 gm/cc).

Particle material	Solid particle size (microns)	Particle density (spg)	Settling velocity (in/sec)		Average settling time (hrs.)*	
			0 vol% solids**	2.46 vol% (3.05wt%) solids	0 vol% solids**	2.46 vol% (3.05wt%) solids
MST	4	2.765	0.00061	0.00045	16.0	21.7
	5	2.765	0.00095	0.00070	10.3	13.9
KTPB	10	1.18	0.00039	0.00029	25.2	34.0
	40	1.18	0.00618	0.00458	1.6	2.1
Sludge	10	1.20	0.00043	0.00032	22.7	30.6
	16	1.20	0.00110	0.00081	8.9	12.0

Note:* Average time for solid particle to travel 35 inch distance from the middle of tank liquid height to the tank floor under a stagnant slurry fluid containing a given amount of solid contents

**Stagnant fluid medium containing single particle

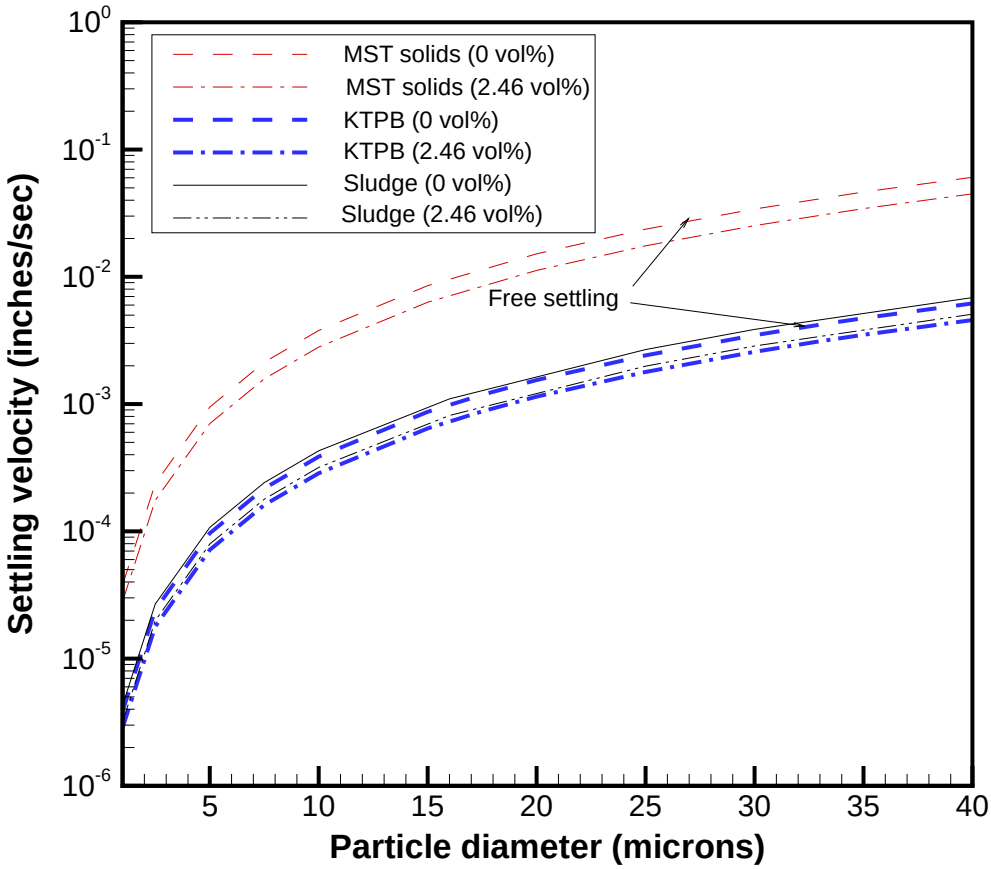

Figure 5. Particle settling velocity as function of particle sizes for different solid contents in a slurry.

3.3 MIXING CRITERION FOR SLUDGE PARTICLES IN TANK 48

As discussed in the previous section, the criteria by which turbulent jet flows entrain and mix sludge particles from the settled solids layer were established by using minimum velocity magnitude required to pick up the particles. The minimum hydraulic force derived by the velocity criterion, which is just sufficient to pick up solids from the settled sludge layer, is referred to as a critical scouring velocity in the literature [Lee et al, 2008]. It will be a function both of the particle properties and of their operating conditions.

As another potential criterion, turbulent eddies related to the turbulent energy dissipation rate disrupt the viscous sublayer and impinge directly on the surface of the solids, which were already suspended by fluid motion [Dimenna and Lee, 2010]. Thus, eddies created by energy dissipation tend to drive turbulent mixing over the flow domain of the tank. For the present analysis, it is suggested that when quasi-steady flow patterns established by jet pumps can suspend particles, then hydrodynamic force associated with local velocity magnitude shears and transports the solids from the solids layer to the bulk liquid domain.

3.4 TANK 48 MODEL AND ASSUMPTIONS

Figure 1 shows geometrical configurations and three-dimensional modeling domain as modeled in the CFD environment for the multi-pump simulations including the internal flow obstructions. Two CFD modeling approaches were taken to evaluate flow patterns for the assessment of different combinations of pump configurations and to estimate insoluble solids concentrations near the transfer pump. One is a single-phase approach to evaluate the flow patterns for a range of different pump configurations. The single-phase modeling calculations were performed by using FLUENT code. The other is two-phase approach considering two phases of fluid and solids for the quantitative estimate of insoluble solids concentration before transfer to the waste feed tank in FBSR process. The two-phase modeling calculations were performed by CFX code, considering both phases of solids and fluid components to be governed by Eulerian motions. Both approaches were taken for the steady-state modeling conditions. For the modeling simulations, a series of the CFD calculations was performed with four pumps for a steady-state flow pattern established near the inlet location of the transfer pump.

Physical model assumptions and geometrical simplifications are listed as follows:

- There are no solid obstructions in the tank other than tank wall, major pump support structures, and one central support column as shown in Fig. 1. The cooling coils were not included in the modeling domain.
- Each slurry pump is simulated to be stationary for the modeling calculations.
- The working liquid is water at 20 ^{o}C. A temperature slightly different from this value will not have a significant effect on flow patterns.
- The liquid region is bounded by a frictionless surface with slip boundary.
- The model is isothermal. No energy equation is calculated.
- The flow in the entire model domain is assumed to be turbulent to give a reasonable representation of the liquid jet leaving the pump nozzle.
- The wavy motion of the free surface due to the interaction with the discharge jet is neglected. Literature data [10] show that the surface wave effect is negligible when the ratio of liquid height above the nozzle to nozzle diameter is larger than 2.5. For a slurry mixer in Tank 48, the ratios are about 31 for the 70 inch liquid level case and about 6 for the 29 inch level.
- Each of the three different solids present in the tank liquid consists of uniform spherical particle with mean diameter.
- For the two-phase initial conditions for the discontinuous solid phase, the total solid volume corresponding to 3.05 wt% is homogeneously formed as a loosely-packed porous layer settled on the tank floor. It consists of three different solids, which are MST, KTPB, and sludge particles.
- For the two-phase modeling calculations, the interfacial drag forces between the continuous fluid and discontinuous solid phases were considered by using
  - Schiller Naumann model for the drag force
  - Lift force with lift coefficient (C_L = 0.5)

- Lopez de Bertodano model with Turbulent Dispersion Coefficient (0.1) for turbulence dispersion
- Virtual mass effect with virtual mass coefficient for spherical shape, $\mu_m = 0.5$
- Wall lubrication force
- Enhanced turbulence production model by Sato Enhanced Eddy Viscosity
- No slip boundary at the solid-fluid interface

The flow conditions for the pump operations are assumed to be fully turbulent since Reynolds numbers for typical operating conditions are in the range of 10^6 based on the pump nozzle conditions. A standard two-equation turbulence model, the κ–ε model [17], was used since benchmarking results against literature data [18] showed that the κ–ε model predicts turbulent flow evolution in a large stagnant fluid domain with reasonable accuracy. The previous results show that although Reynolds stress model has the potential to give more accurate results for flows in which streamline curvature, swirl, rotation, or rapid changes near the wall boundary might be important, the standard κ–ε model is considered a good model for mixing calculations over a large fluid domain such as Tank 48. This model specifies the turbulent or "eddy" viscosity μ_t by the empirical equation.

$$\mu_t = \left(\frac{C_\mu \rho_f k^2}{\varepsilon} \right) \tag{15}$$

In the present calculations, C_μ is 0.09 [17]. The turbulent viscosity is computed by solving two transport equations for turbulent kinetic energy (k) and dissipation rate of turbulent energy(ε). The governing equations to be solved include one continuity equation, three momentum equations for the three component directions (x, y, and z directions), and two modeled transport equations for the two turbulence quantities, namely κ and ε. Water was used to simulate the fluid in the tank assuming that it would give an acceptable representation of the flow patterns. The sensitivity studies were previously performed using typical slurry fluid properties for an indexed pump model, i.e., the pump in a fixed radial direction.

Three-dimensional steady-state numerical simulations are made for the Tank 48 modeling analysis by taking two modeling approaches. One approach is the single-phase tank model to estimate the flow patterns for various indexed pump orientation and number of operating pumps. The calculated flow patterns are applied to estimate the solid suspension area by using the minimum solid suspension velocity established in the previous section. The other approach is the two-phase tank model to calculate the solid concentrations over the entire fluid domain of tank 48.

The modeling domain defined for the modeling analysis is shown in Fig. 6. Typical computational meshes established for the CFD simulations are shown in Figs. 7 and 8. The number of the established computational meshes for the entire tank domain ranges from 2 x10^6 to 3 x 10^6 nodes. This number was established from sensitivity studies of computational meshes. Mesh density is significantly higher in the vicinity of the pump discharge to capture the flow behavior relative to the nozzle diameter. The characteristic mesh dimension is much greater in regions far from the nozzle and other solid structures to keep the total number of nodes manageable.

Range of different indexed jet directions of four slurry pumps were considered to perform the sensitivity calculations for the flow patterns with respect to the baseline jet directions, Case

1, as shown in Fig. 9. Combinations of different pump orientations used for the steady-state pump model are illustrated in Fig. 9.

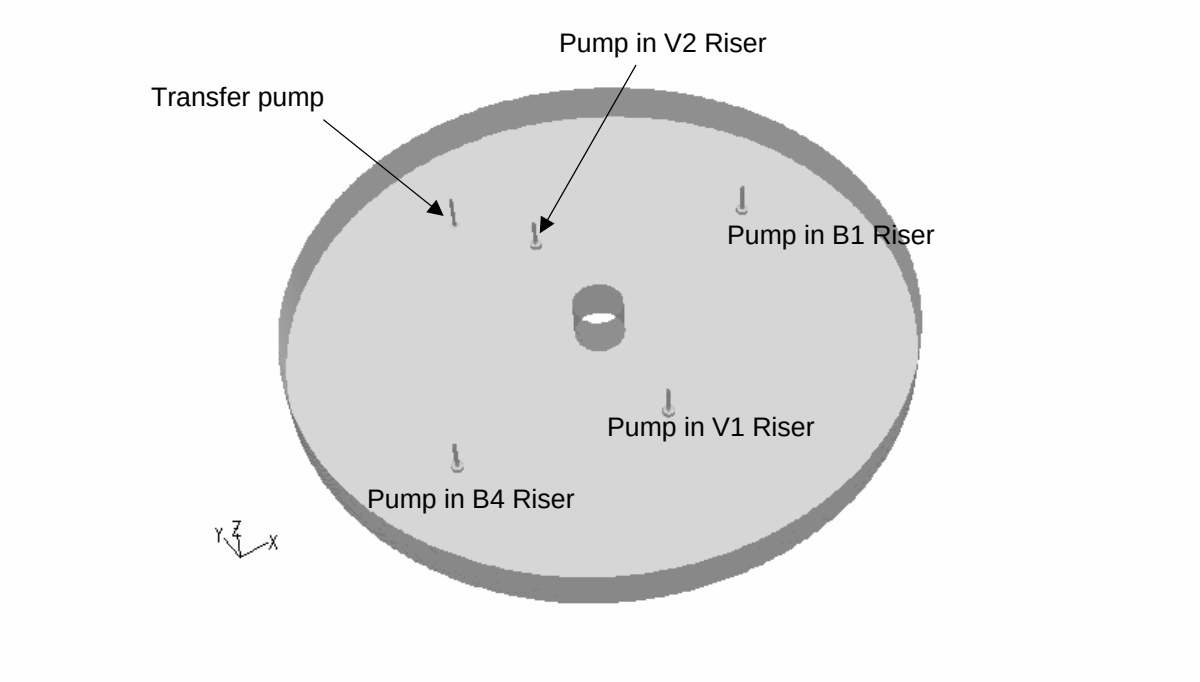

Figure 6. Computational domains of the tank model without cooling coils for the CFD analysis

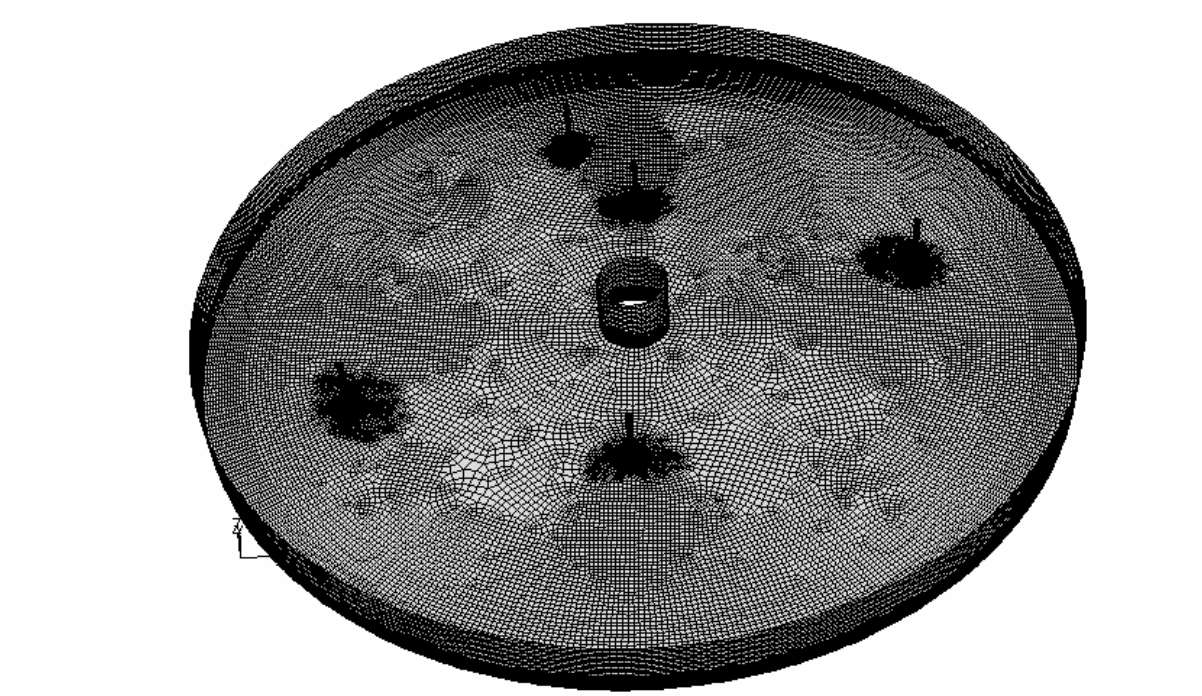

(Volume mesh for the three-dimensional tank domain)

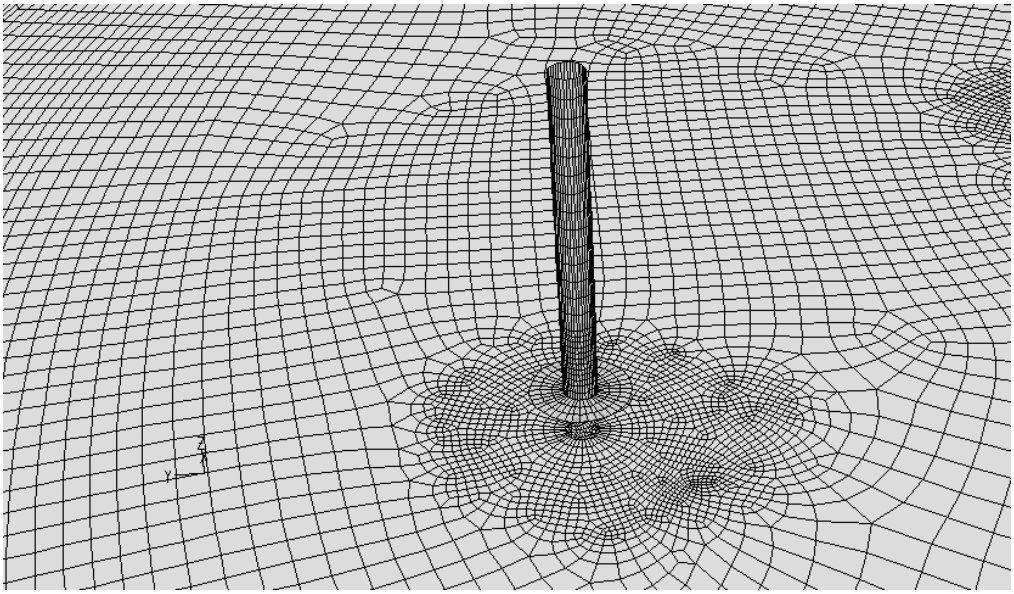

(Representation of the refined mesh near pump)

Figure 7. Computational volume meshes and representative two-dimensional meshes used for the single-phase tank model with four mixing pumps and one transfer pump

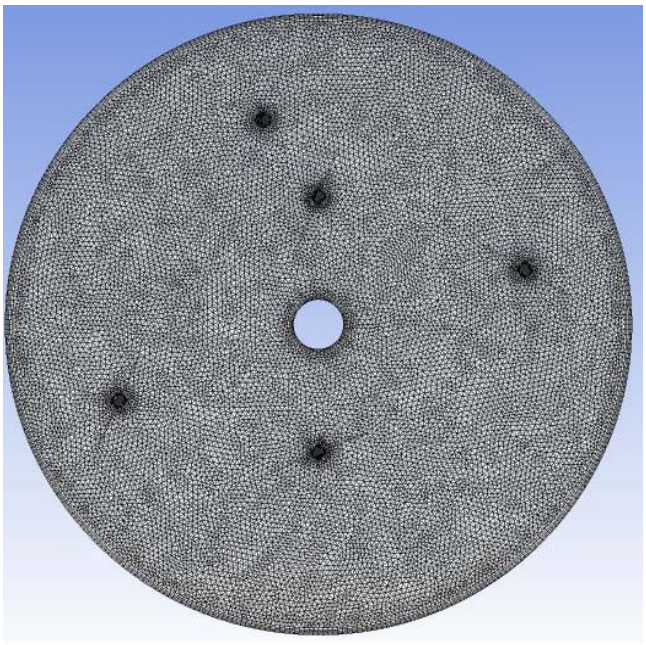

(Mesh for the three-dimensional tank domain)

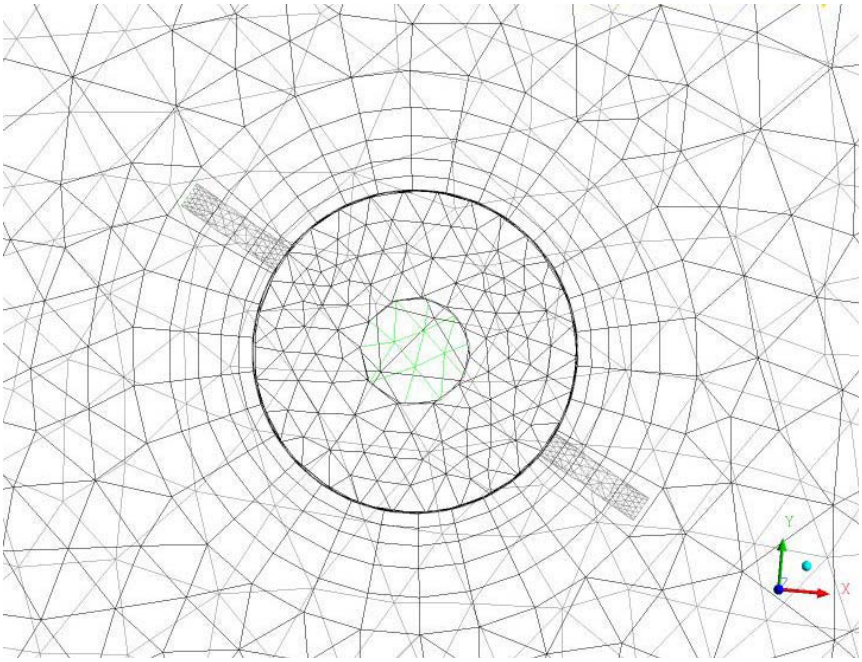

(Representation of the refined mesh near pump)

Figure 8. Computational volume meshes used for the two-phase tank model with four mixing pumps and one transfer pump

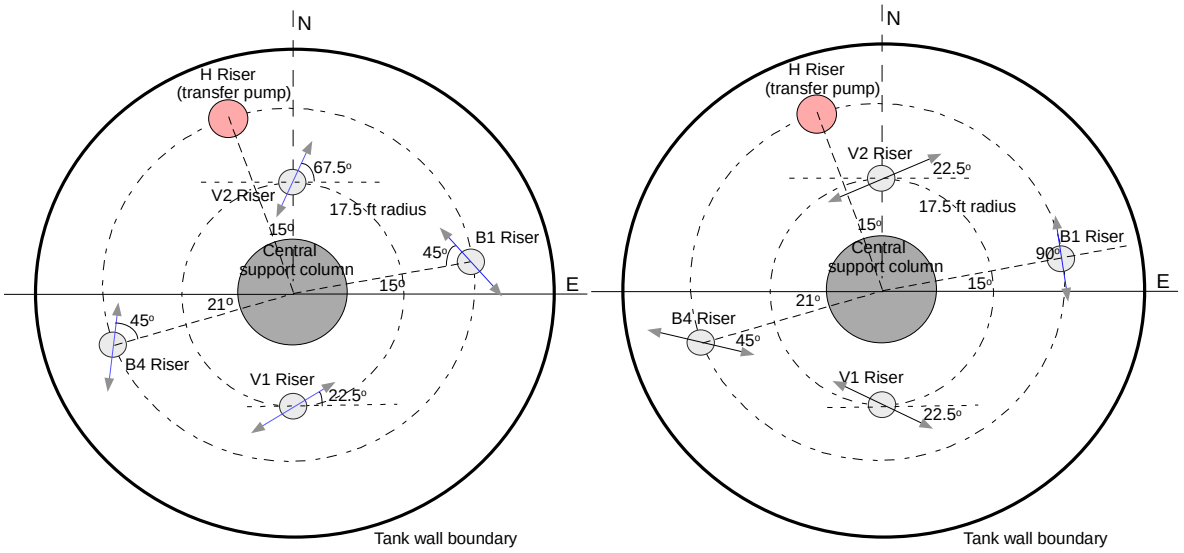

(Case 1: Baseline pump configuration) (Case 2)

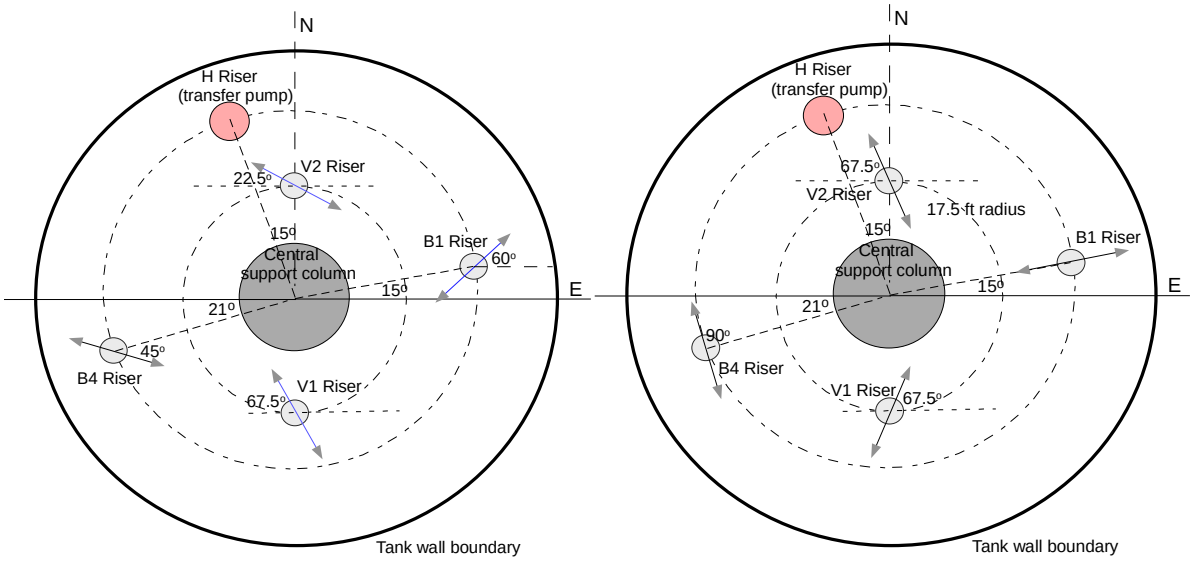

(Case 3) (Case 4)

Figure 9. Different pump orientations considered for the indexed pump models

4.0 RESULTS AND DISCUSSIONS

The Tank 48 models have been developed by a CFD approach to include several internal flow obstructions such as central support column and major pump housings in the flow domain and analyses performed to estimate circulation flow patterns within Tank 48 to evaluate the ability of the slurry pumps to suspend the solids remaining in the tank. The mixing pumps are considered to be stationary for flow pattern estimation of the jet pump. For the CFD modeling calculations, different pump orientations and configurations were considered for examining the impact of mixing performance for the baseline pump configurations. The asynchronous transient effects of pump rotations and number of pump operations on the solids suspension are not addressed in this analysis.

As mentioned previously, the work used two different solution methods for the modeling calculations. One is a single-phase tank model by using the previous method with FLUENT code [Lee and Dimenna, 2008, and Lee et al., 2004] since the model predictions were in good agreement with test data. The other is a two-phase tank model of fluid and solid phases by CFX code to quantify the solid concentrations near the inlet region of the transfer pump, which is located at 9 inches above the tank floor. For the modeling calculations, a prototypic geometry is modeled by the hexahedral and tetrahedral meshes over the computational domain. The modeling domain to be used for the present analysis is presented in Fig. 6. Nominal design and operating conditions of the pumps used in the Tank 48 model are presented in Table 1. Based on the modeling domain and operating conditions, turbulent flow calculations were performed. The three-dimensional model was run in steady state mode for indexed pump operations to allow the jet flow profile to develop steady state flow.

For the single-phase approach, local fluid velocity at any distance from the nozzle is employed as a measure of the slurrying and mixing effectiveness in Tank 48H operations since the flow velocity criterion is used as the primary indicator of the ability to scour insoluble solids and to suspend them, based on the solution method established in the previous section. The single-phase model was used as a primary tool to evaluate flow circulation patterns for the baseline mixing operations of Tank 48H and to perform the sensitivity analyses for different numbers of pumps, and various pump operating conditions such as indexed pump orientations. Figure 9 shows four different cases for various indexed pump orientations considered by the single-phase tank model. The two-phase modeling approach was mainly taken for the quantitative evaluations of the solid concentrations and focused on the baseline pump configurations as shown in Fig. 9. The two-phase modeling results should be considered as preliminary scoping calculations since the model was not validated against test results. Table 6 shows all cases considered for the present modeling analysis.

As discussed earlier, Case 1 was selected as the baseline pump configurations, since four slurry pumps are available at maximum in stirring up the solids settled on the tank floor, and the product $d_o U_o$ for each pump is about 9.5 ft^2/sec as shown in Table 1. Thus, although Case 1 has insufficient flow patterns to suspend and mix the solids, other three configurations in Fig. 9 may satisfy the flow mixing requirement. For an assessment of the impact of different pump combinations on the tank mixing, number of pump failures among the four pumps was considered. In the present analysis, the mixing model with two slurry pumps operated was simulated as the worst scenario since the previous results for the Tank 50 mixing analysis [Lee and Dimenna, 2008] showed that the case with one pump operation did not satisfy the solid mixing requirements.

Table 6. Modeling cases considered for the analysis

Model	Pump configurations (See Fig. 9)	No. of operating pumps	Tank liquid level (inches)	Purposes
Single-phase model	Case 1 (Baseline)	4	70	To evaluate flow patterns for solids mixing requirements
	Case 1 to Case 4	4	70	To perform the impact of indexed pump orientations on flow patterns
	Case 1 (Baseline)	2, 3+	70	To perform the impact of number of pump operations on flow patterns
Two-phase model	Case 1 (Baseline)	4, 3, 2*	70	To estimate quantitative solid concentrations near the transfer pump
	Case 1 (Baseline)	4, 3, 2*	29 (min. tank level)	To estimate quantitative solid concentrations near the transfer pump

Note: +For the three-pump model, the slurry pump at Riser V2 is assumed to be shut off, and for the two-pump model, the two pumps at Risers B4 and V2 are assumed to be shut off
*For the three-pump model, the slurry pump at Riser B4 is assumed to be shut off, and for the two-pump model, the two pumps at Risers B1 and B4 are assumed to be shut off.

In this work, the two-equation turbulence model, k-ε model, was applied to perform the calculations of jet flow into a stagnant liquid medium of about 250,000 gallons equivalent to a 85-ft cylindrical tank with 70 inch tank liquid level since the standard k- ε model is well known to be valid only for very large Reynolds number (i.e., greater than 10^5 Reynolds number). As shown in Table 7, mixing flow conditions correspond to 8.5 x 10^5 Reynolds number in terms of jet diameter and jet discharge velocity. Figure 10 compares the modeling predictions for the steady-state jet velocities along the principal discharge direction inside Tank 48 with the jet test results available in the literature as shown in Table 7.

As shown in Fig. 9, the single-phase baseline model was simulated with four pumps operated to evaluate flow circulation patterns for the solid mixing operations of Tank 48. For the simulations, B1 and B4 pumps are located at 16.81 inches above the tank floor, and V1 and V2 pumps located at 19.81 inches. Figure 11 compares the results for the flow patterns at the B1-B4 pump discharge plane among the four different pump orientations under the same color scaling system. Dark blue areas in the figure indicate the stagnant fluid zone, noting that the red color has the flow velocity magnitude larger than 1 m/sec. When the jet discharge flows are directly interacted as shown in the pump orientations of Case 4, flow patterns are not efficient in terms of the solid mixing requirement.

As shown in Table 3, the MST particle requires the largest local velocity magnitude of 0.053 m/sec (0.173 ft/sec) among the three different solid particles of MST, KTPB, sludge, which are present during the mixing operations in Tank 48. For the conservative estimate, flow

patterns driven by the slurry jets are evaluated in terms of the MST suspension velocity criterion. When four slurry pumps are operated for the solids mixing, the red areas of the MST suspension region at the horizontal plane of transfer pump inlet are compared for various combinations of jet orientations in Fig. 12, noting that the non-red region has local velocity magnitude smaller than the minimum velocity required for suspending 5-micron MST solids. The modeling results show that the flow patterns driven by four pump operation satisfy the solid suspension requirement.

When V2 pump is not used for the mixing operation, the flow patterns generated by the three pump operations are compared for various combinations of pump orientations in Fig. 13. The red zones of the MST suspension regions, which are driven by the three pump operations, are compared for the four different flow patterns in Fig. 14. The results show that when one of the four pumps is not operated, the flow patterns are qualitatively satisfied with the minimum suspension velocity criterion as shown in Table 3.

When only two slurry pumps of the four-pump baseline orientations, Case 1, are operated, Figure 15 shows the velocity magnitude at the horizontal plane crossing the jet discharge exit of the slurry pumps at Risers B1 and B4 during a steady state operation, noting that the red region has local velocity higher than 1 m/sec. For the same operating conditions, the velocity contour plots at the horizontal plane crossing the inlet region of the transfer pump at Riser H are shown in Fig. 16. In the figure, the red zone has local velocity magnitude higher than 0.053 m/sec, which is required to scour and transport 5-micron MST solids. The modeling results show that there is insufficient flow to keep MST solids suspended at the transfer pump inlet throughout the horizontal tank domain as shown in Fig. 16.

Figure 17 qualitatively compares steady-steady snapshots of flow velocity magnitudes for various number of slurry pumps operated under the baseline pump configurations at the horizontal plane crossing the inlet region of the transfer pump. In the figures, the red zone has local value higher than 1 m/sec. The MST suspension regions at the inlet region of the transfer pump are qualitatively compared under various pump combinations in Fig. 18. The results show that when two slurry pumps located at Risers B1 and V1 are operated in Tank 48, local velocity magnitudes near the inlet of transfer pump reach at most about 0.1 m/sec. Based on the modeling results, it is shown that the two-pump case does not provide sufficient mixing results for the tank contents containing MST, KTPB, and sludge solids. When the tank contents consist of sludge solids, the two pump case provides sufficient local velocities to suspend the sludge particles as shown in Fig. 19.

The single-phase model was simulated to evaluate flow circulation patterns for the solid mixing operations of Tank 48 in a qualitative way for a computational efficiency. The model was also used to conduct sensitivity calculations to evaluate the impacts of different numbers of operating pumps and various pump orientations on the mixing performance.

The two-phase model was developed by taking an Eulerian approach to estimate the solid concentrations over the entire tank domain in a quantitative way. The modeling calculations were performed for the baseline pump orientations, Case 1, as defined in Fig. 9. As mentioned earlier, the modeling validation is not addressed here since it is beyond the current scope of work.

All two-phase modeling calculations are performed assuming that all solids inside Tank 48 are settled on the tank floor with loosely packed layer before the initiation of the slurry pump operations, and they consist of uniform spherical size of 40 micron diameter. Figure 20

presents the KTPB weight percentage contours at the horizontal plane of different elevation levels for the four-pump baseline configurations with 70 inch tank liquid level, noting that the red region has the weight percentage higher than and equal to the average value of 2.01 wt%. When the all four pumps are oriented at the directions rotated by 90^{o} with respect to the baseline configurations as shown in Fig. 9, the KTPB solid concentrations at the four different elevations of 0.2 inches (near tank floor), 9 inches (transfer pump inlet) , 22.6 inches, and 70 inches (top liquid surface) are shown in Fig. 21. The results indicate that the solid concentrations near the transfer pump inlet at Riser H are higher than the average concentrations of 2.01 wt% under the four pump operations.

As shown in Table 2, the total insoluble contents to be modeled for the Tank 48 mixing analysis are 3.05 wt%, resulting in 0.15 wt% contents for MST solids. Figure 22 shows the MST weight percentage contours at the horizontal planes of the four different elevations for the four-pump baseline configurations with 70 inch tank liquid level. For the same pump operating conditions, the solid concentrations for the 16-micron sludge particles at the four different elevations are shown in Fig. 23.

As shown in Table 2, KTPB particles have the largest weight percentages among the three different kinds of insoluble solids to be mixed for the Tank 48 mixing analysis, while MST has the smallest concentration in the tank but the largest density. When the operating pumps are reduced from the maximum four pumps to two pumps, Figure 24 compares the KTPB weight percentage contours at the horizontal planes of transfer pump inlet elevation for the baseline pump orientations under 70 inch tank liquid level. The red color in the figure indicates local concentration higher than and equal to the homogeneously averaged value, 2.01 wt%. Figure 25 shows the MST concentration contours at the horizontal planes of four different elevation levels for the two-pump baseline configurations with 70 inch tank liquid level. The results show that when two pumps are operated for the tank mixing, about 20 % for KTPB and about 50% for MST of the entire cross-sectional tank space have local solid concentrations smaller than the tank-averaged value at the elevation of the transfer pump inlet, respectively.

The sensitivity calculations for different tank liquid levels were conducted to examine the impact of tank level on the solid mixing performance for given pump configurations. When tank level is changed from the baseline value of 70 inches to the minimum level of 29 inches for the four pump operations, Figure 26 shows the KTPB concentration distributions for the horizontal planes crossing four different elevations of 0.2 (near tank floor), 9 (transfer pump inlet) , 22.6, and 29 inches (top liquid surface). For the same modeling conditions, the solid concentration distributions for the MST and sludge particles are shown in Figs. 27 and 28, respectively. The red regions in the figures have local solid concentrations higher than and equal to the averaged values of 2.01 wt% for KTPB, 0.15 wt% for MST, and 0.89 wt% for sludge.

When two slurry pumps are used for the tank mixing operation with a minimum liquid level of 29 inches, the KTPB and MST solid concentration distributions at the four different elevations are shown in Figs 29 and 30, respectively. The results show that for the two-pump operation, the solid concentrations at and above the 9 inch elevation of the transfer pump inlet are non-uniformly distributed, and they are lower than the tank-averaged value. When number of the operating pumps for the mixing process is varied from the maximum four pumps to two pumps, Figures 31 and 32 compares the KTPB and MST concentrations averaged over the entire cross-sectional area of each selected elevation along the vertical liquid height of the 70 inch tank liquid level for three different pump operating conditions,

respectively. For the 29 inch tank liquid level with the same operating pump conditions, the area-averaged KTPB solid concentrations are compared for three different cases of number of operating pumps along the vertical liquid height in Fig. 33. The two-phase results for different number of pump operations and different tank liquid levels are quantitatively compared in Table 8 and Table 9.

The sensitivity results show that when the modeling calculations assume that the solids are initially settled down on the tank floor in a loosely-packed layer, the wall boundary layer region has a steep concentration gradient with respect to the layer thickness, but the upper half region of the tank liquid has the solid concentrations lower than the tank-average value. As shown in the figures, when more slurry pumps are operated for the tank mixing, the solid mixing efficiency is improved significantly in terms of local solid concentration as expected. It is noted that as tank liquid level is reduced from the highest level of 70 inch to the minimum level of 29 in, the solid concentrations become more uniform from the comparison of the results shown in Figs. 31 and 33. These results are consistent with the literature results since the ratio of the power supply to the mixing volume becomes larger [Lee et al, 2008, and Tatterson, 1991].

Figure 34 compares the KTPB concentrations averaged by the volume above the transfer pump inlet plane as function of number of operating pumps for two different tank liquid levels of 70 and 29 inches, noting that the overall average concentration of KTPB soilds in Tank 48 is 2.01 wt%. The solid concentrations for the heaviest particle such as MST are compared for the two different tank levels and number of operating pumps in Fig. 35. In the same way, total insoluble solid concentrations are quantitatively compared for each of the pump operating conditions in Fig. 36. When the number of operating pumps is reduced by two, the MST solid concentration for the region above the transfer pump inlet (9 inch elevation) is decreased by about 27% in terms of the weight percentage. For the same number of operating pumps, the solid concentration for the 70 inch liquid level is at most 4% smaller than the 29 inch liquid level case. The results clearly indicate that the number of the pumps operated for the mixing is a dominant factor in getting better mixing of the tank solids.

Table 7. Data conditions of turbulent jets used in Fig. 10

Authors	Jet diameter (mm)	Fluid	Reynolds number, Re_{jet}
SRS Tank 48	41	Water	850,000
Kiser (1963)	9.525	Water	35,000
Post (1998)	10	Air	10,000

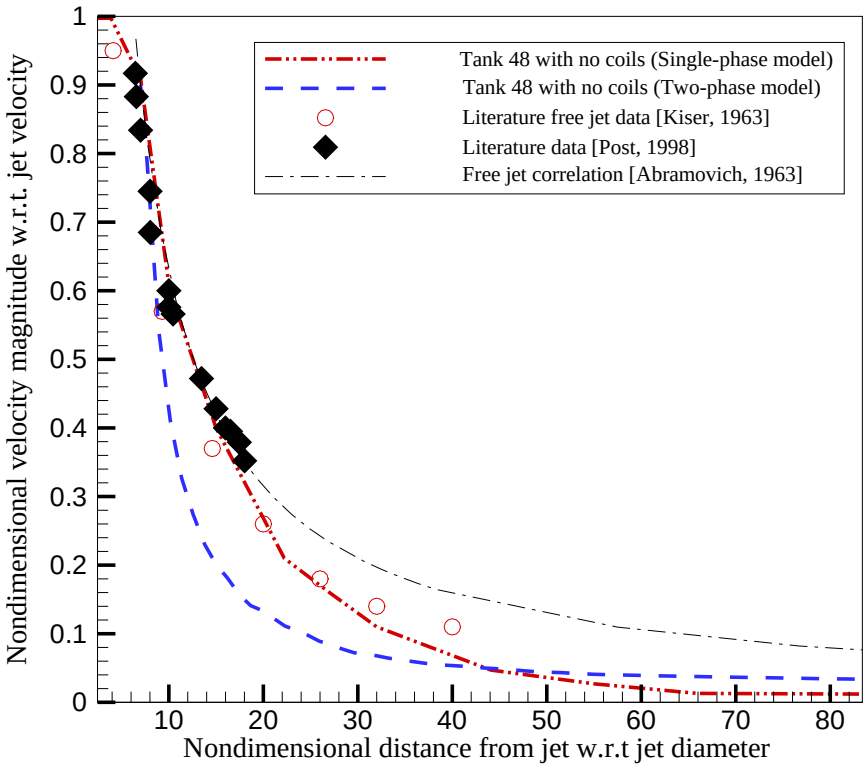

Figure 10. Comparison of steady state flow velocity of the mixing jet with the literature data along the principal discharge line inside Tank48 with no coils

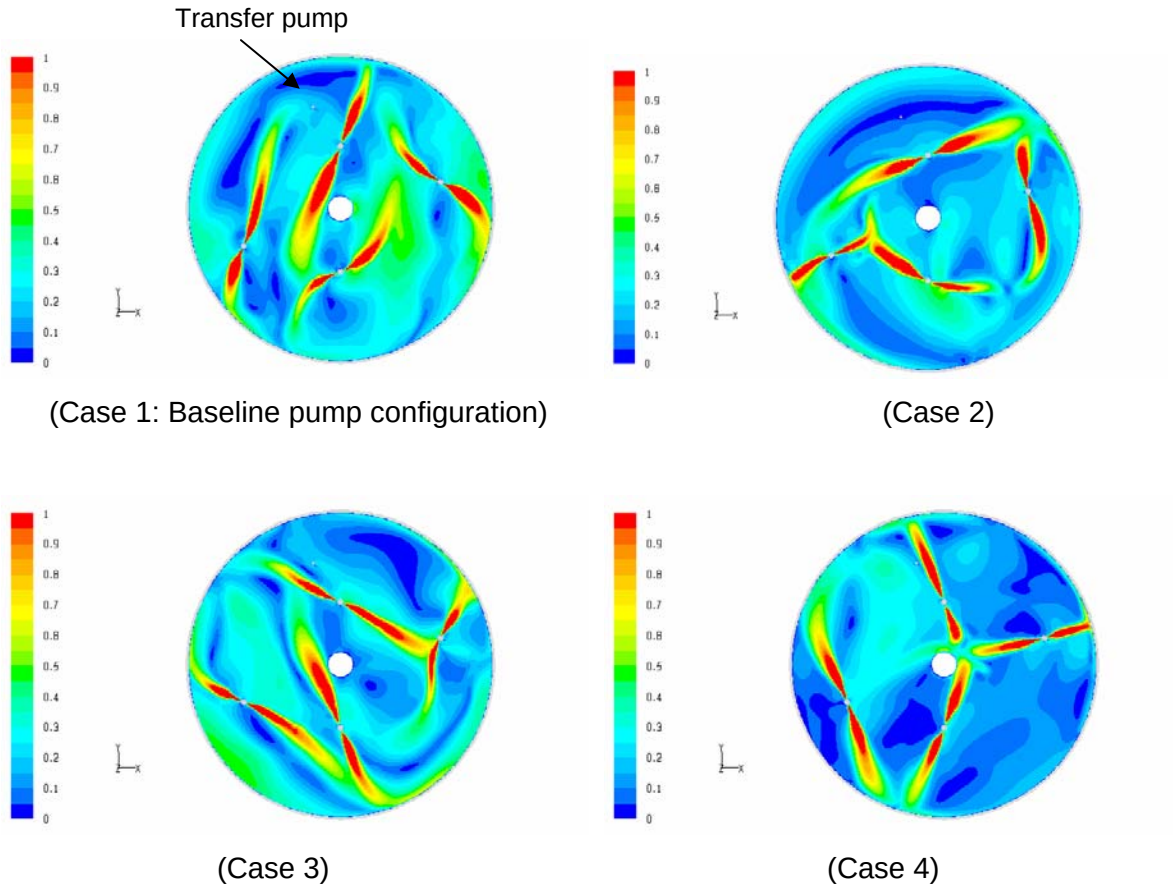

Figure 11. Comparison of flow patterns at the B1-B4 jet discharge plane for various jet directions under 4 pump operations, indicating that the red region has local velocity magnitude larger than 1 m/sec.

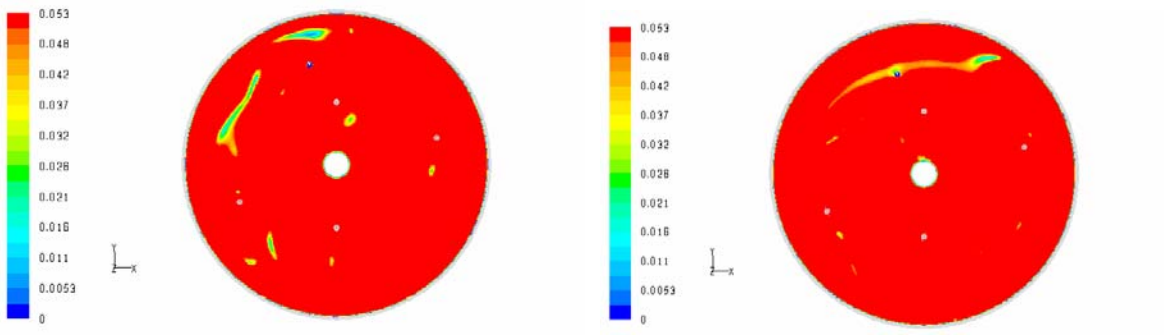

(Case 1: Baseline pump configuration) (Case 2)

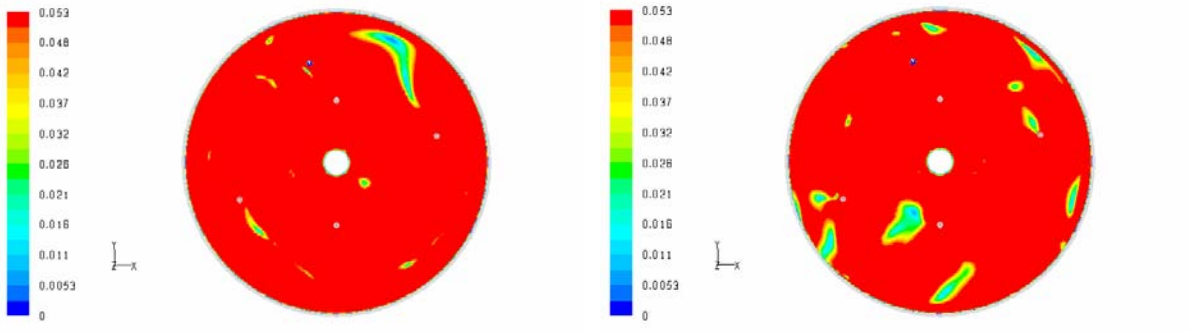

(Case 3) (Case 4)

Figure 12. Comparison of flow patterns at the transfer pump inlet plane for various jet directions under 4 pump operations, indicating that the red region has the MST in suspension.

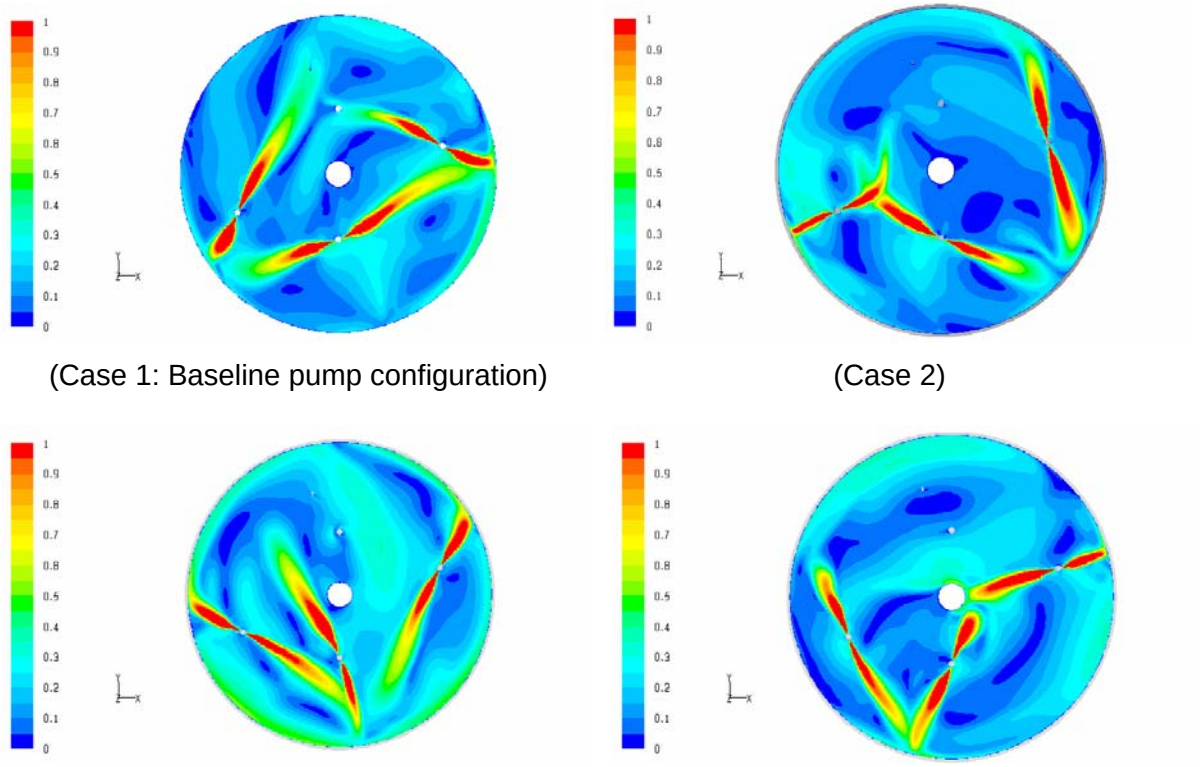

(Case 1: Baseline pump configuration) (Case 2)

(Case 3) (Case 4)

Figure 13. Comparison of flow patterns at the transfer pump inlet plane for various jet directions with 3 pumps in operation and V2 pump off, indicating that the red region has local velocity magnitude larger than 1 m/sec.

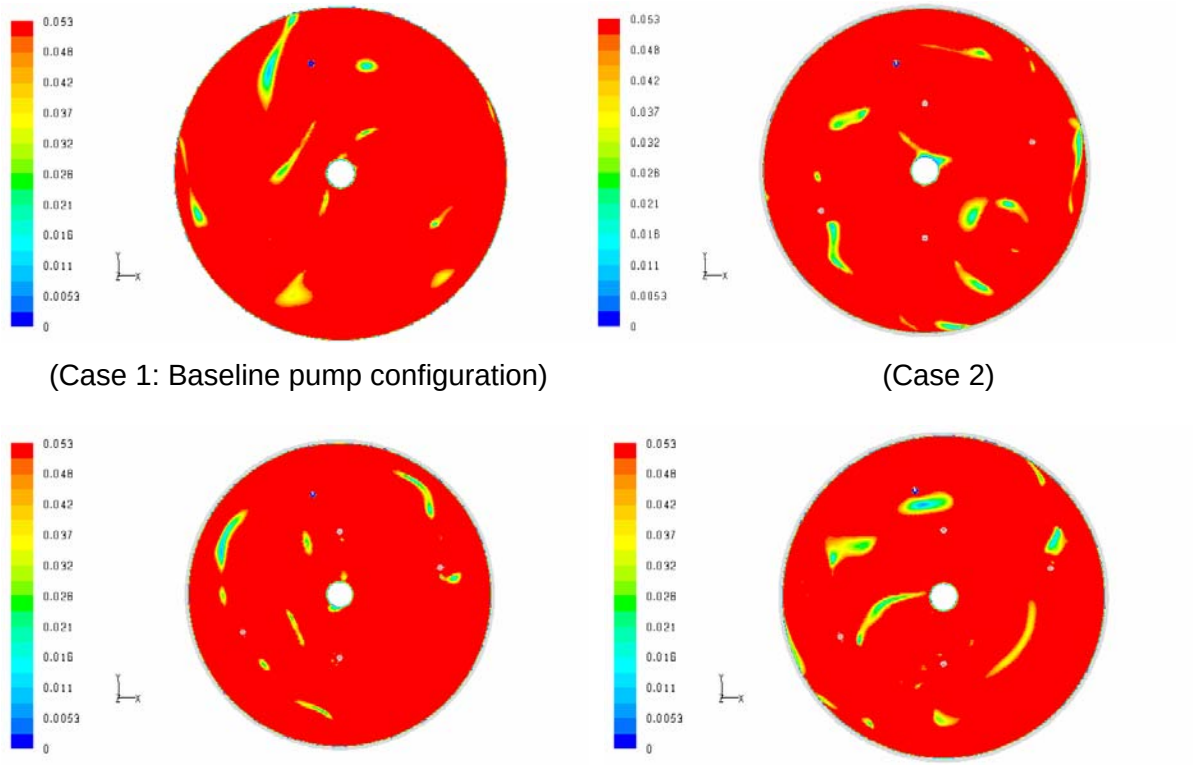

Figure 14. Comparison of flow patterns at the transfer pump inlet plane for various jet directions under 3 pump operations with V2 pump off, indicating that the red region has the MST in suspension.

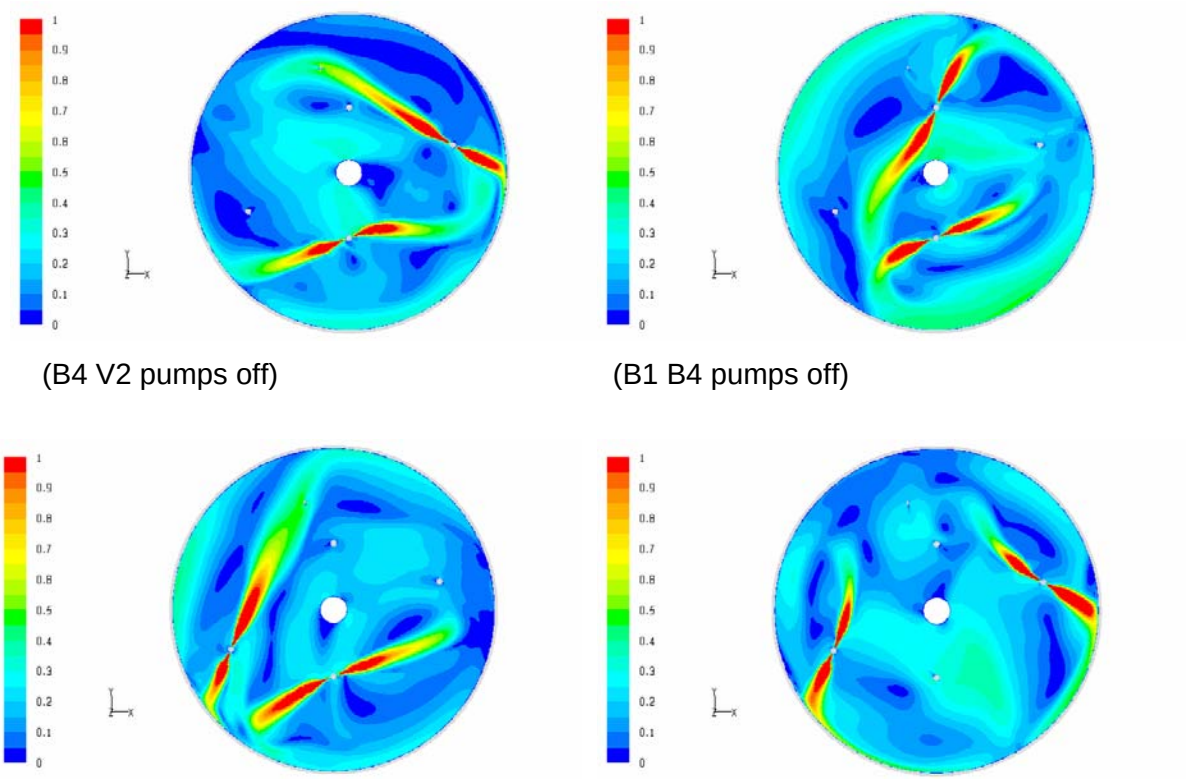

Figure 15. Comparison of flow patterns at the transfer pump inlet plane for various jet directions under 2 pump operation with the baseline configuration. The red region has >1m/sec local velocity magnitude.

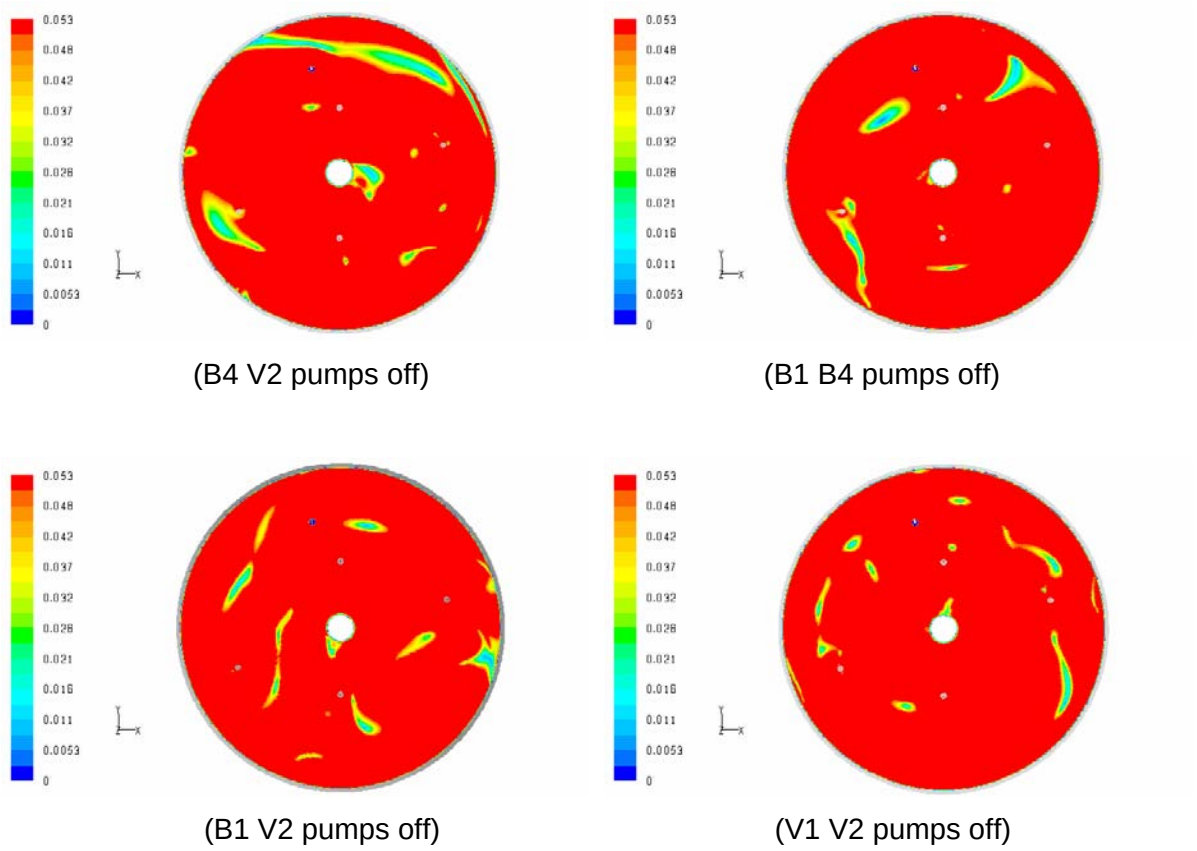

Figure 16. Comparison of flow patterns at the transfer pump inlet plane for various jet directions under 2 pump operations with the baseline configurations, indicating that the red region has the MST in suspension.

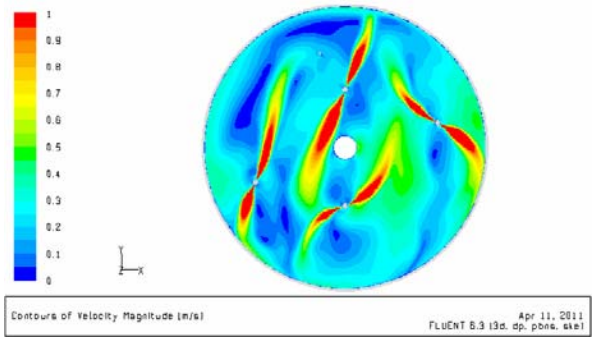

(4 pumps operated)

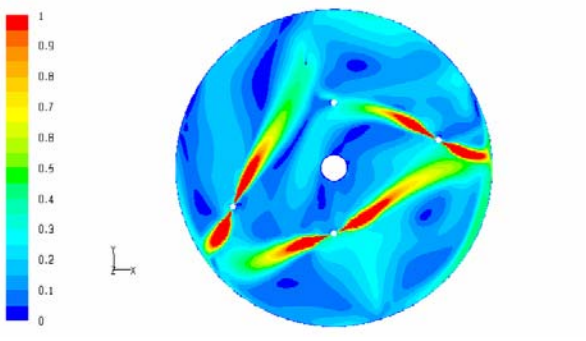

(3 pumps operated: V2 pump off)

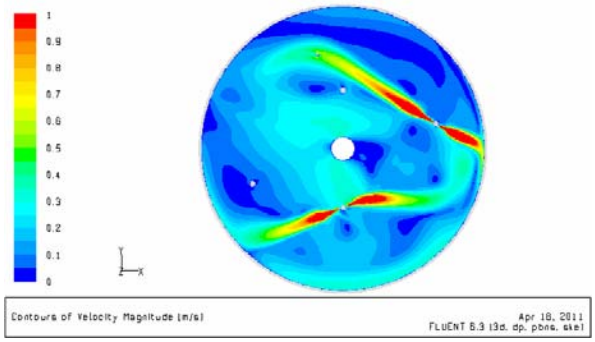

(2 pumps operated: B4 and V2 pumps off)

Figure 17. Comparison of flow distributions at the B1-B4 pump discharge plane for various pump operating conditions of the baseline pump configurations, indicating that the red region has local velocity magnitude larger than 1 m/sec.

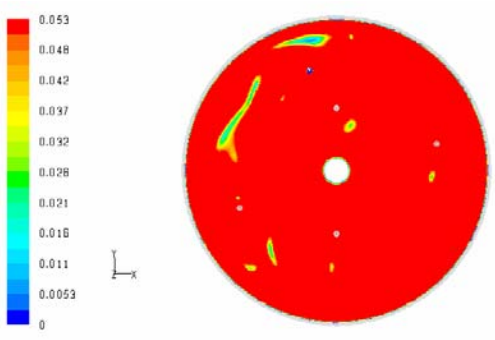

(4 pumps operated)

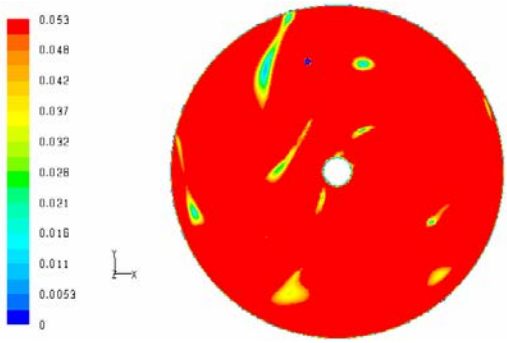

(3 pumps operated: V2 pump off)

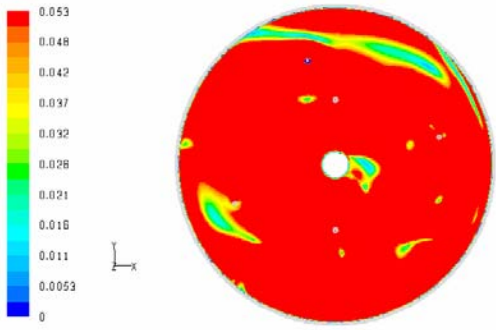

(2 pumps operated: B4 and V2 pumps off)

Figure 18. Comparison of MST suspension regions for various pump operating conditions of the baseline pump configurations (Case 1), indicating that the red region has the MST solids suspended.

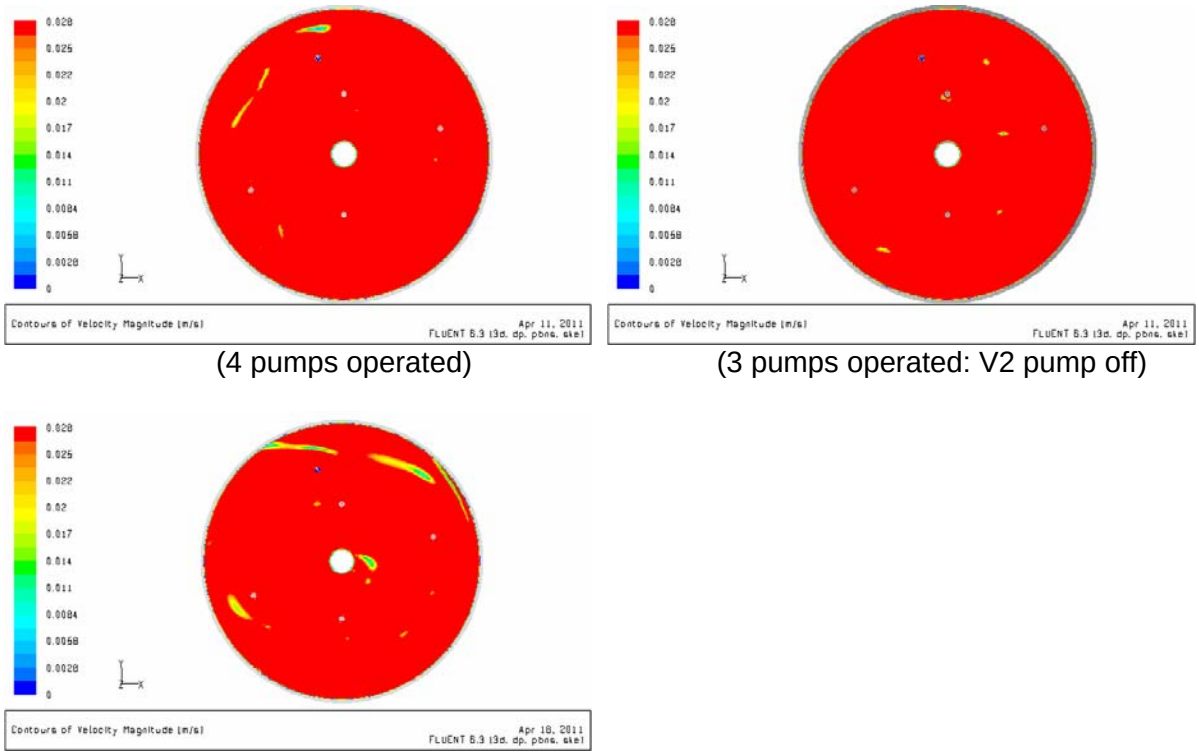

(4 pumps operated) (3 pumps operated: V2 pump off)

(2 pumps operated: B4 and V2 pumps off)

Figure 19. Comparison of sludge suspension regions for various pump configurations, indicating that the red region has local velocity larger than the minimum sludge suspension velocity, 0.028 m/sec.

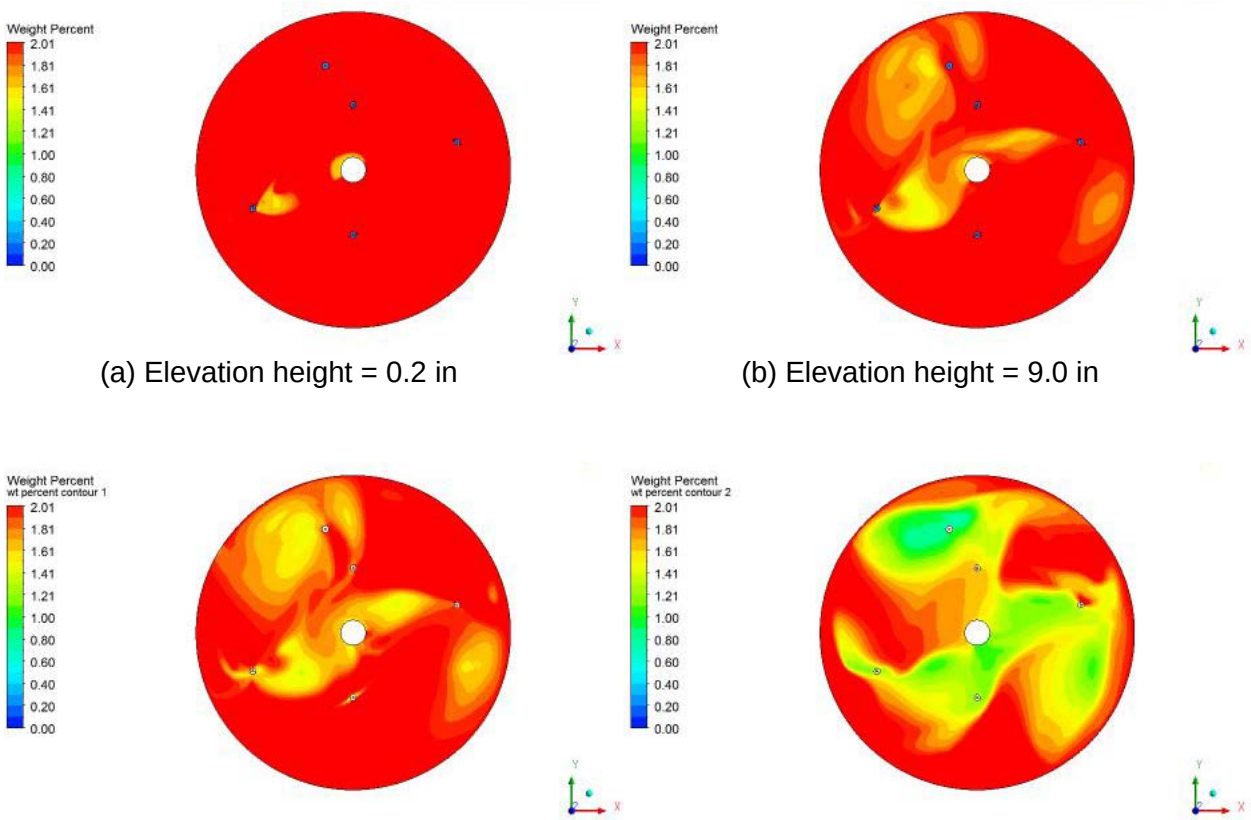

(a) Elevation height = 0.2 in

(b) Elevation height = 9.0 in

(c) Elevation height = 22.6 in

(d) Elevation height = 70.0 in

Figure 20. KTPB weight percentage contours at the horizontal planes of different elevation levels for the four-pump baseline configurations with 70 inch tank liquid level

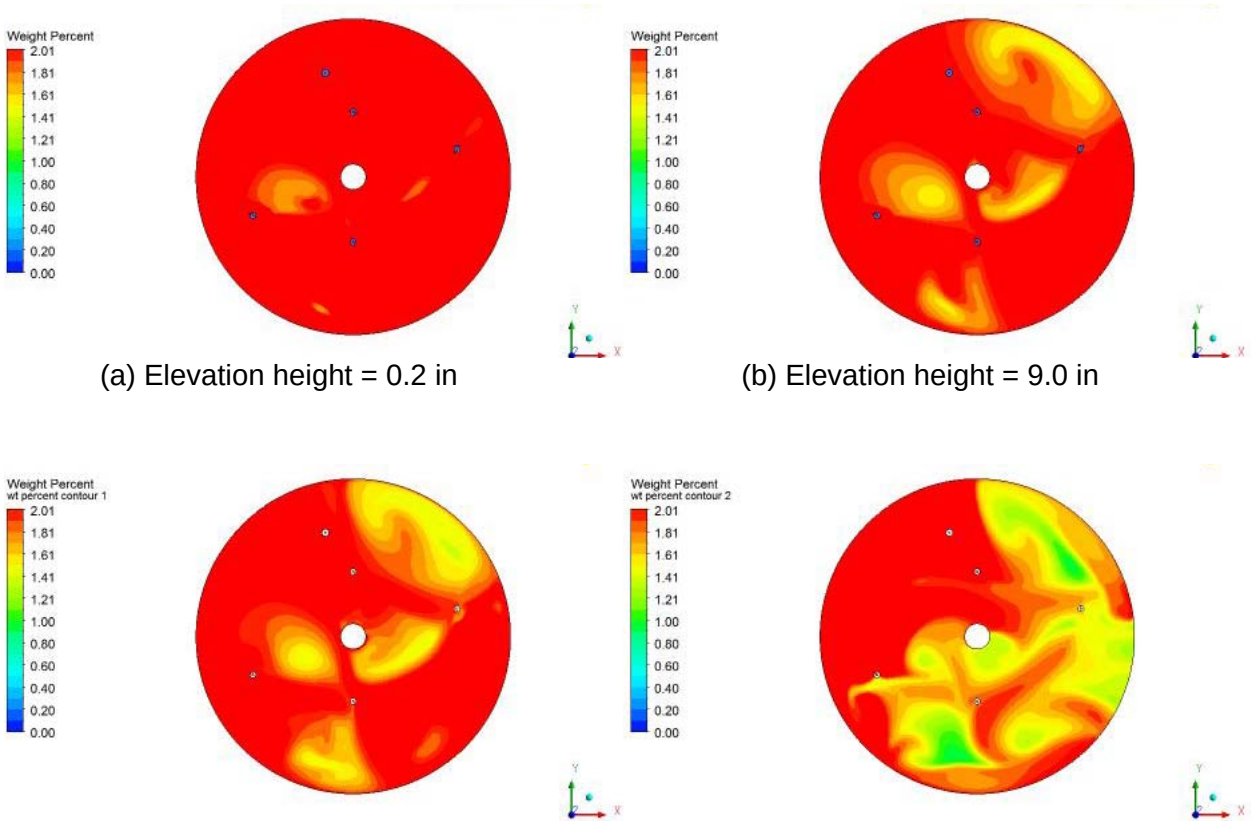

(a) Elevation height = 0.2 in

(b) Elevation height = 9.0 in

(c) Elevation height = 22.6 in

(d) Elevation height = 70.0 in

Figure 21. KTPB weight percentage contours at the horizontal planes of different elevation levels for the pump configurations of Case 3 with 70 inch tank liquid level

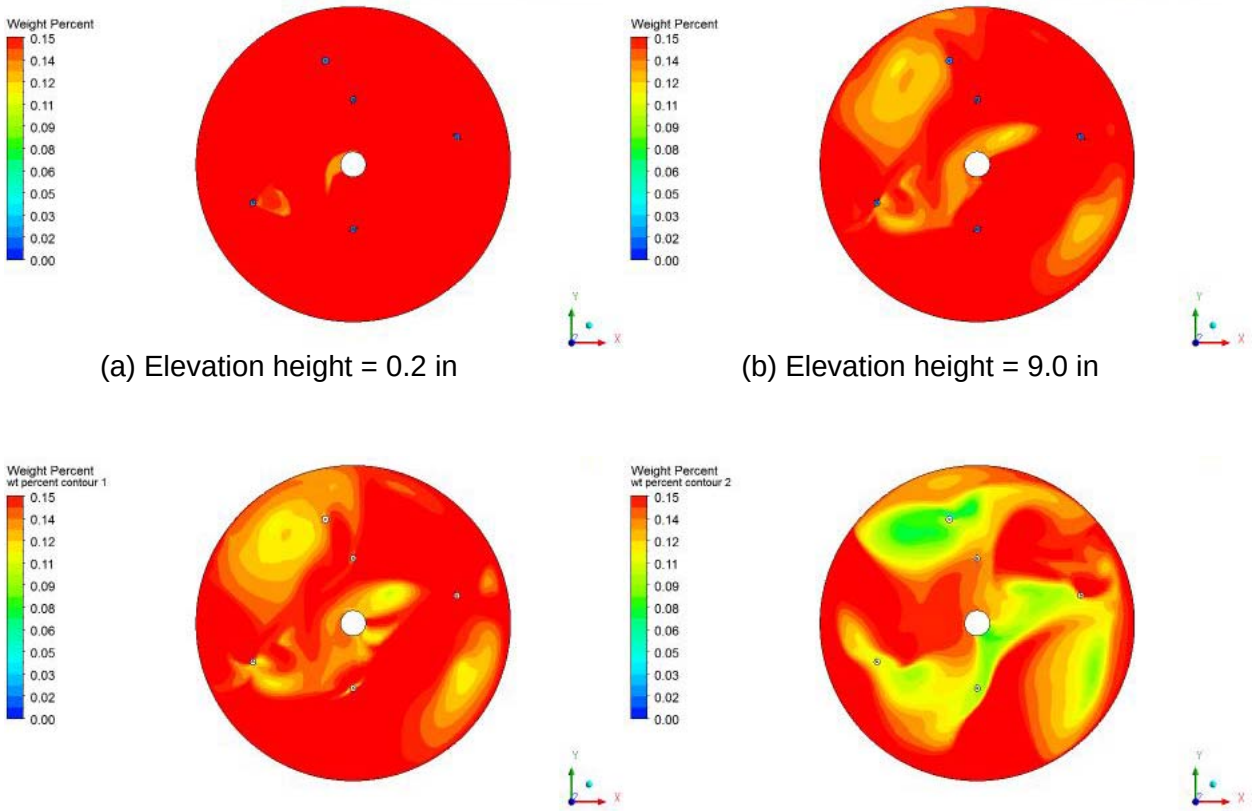

(a) Elevation height = 0.2 in

(b) Elevation height = 9.0 in

(c) Elevation height = 22.6 in

(d) Elevation height = 70.0 in

Figure 22. MST weight percentage contours at the horizontal planes of different elevation levels for the four-pump baseline configurations with 70 inch tank liquid level

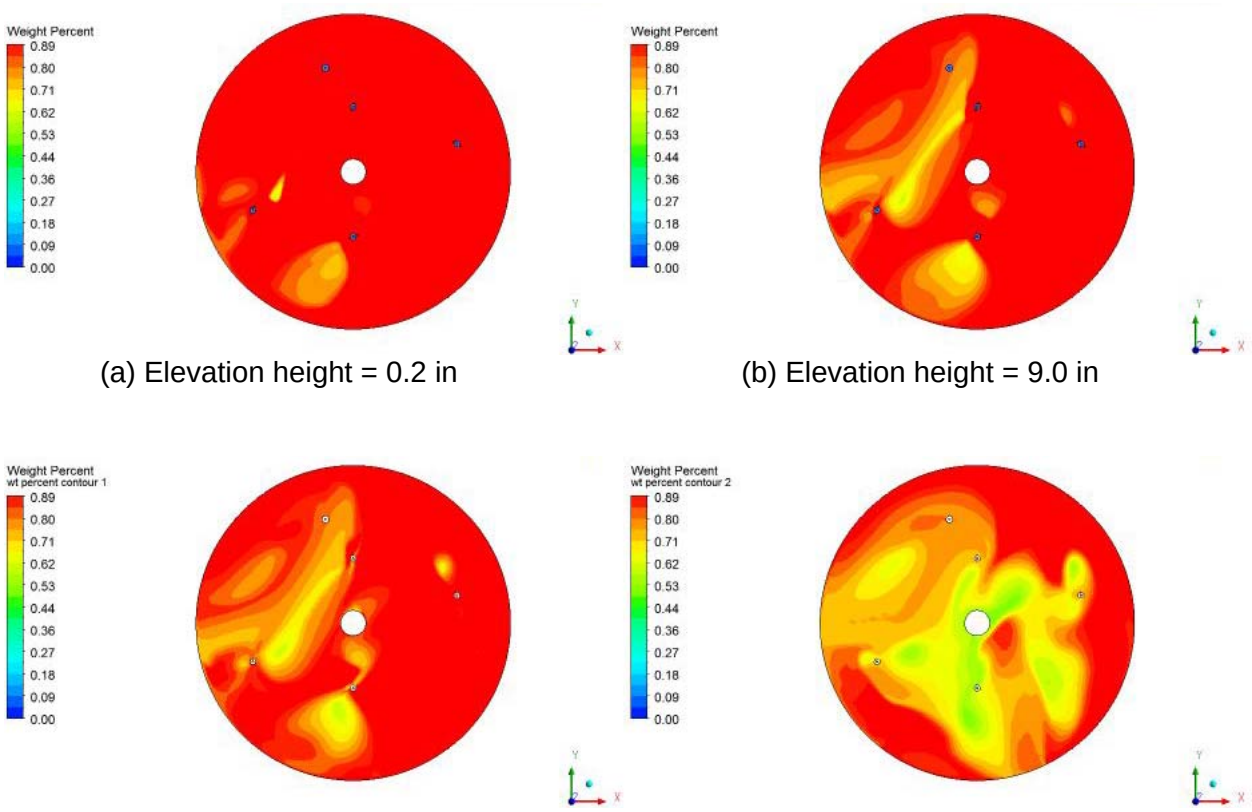

(a) Elevation height = 0.2 in

(b) Elevation height = 9.0 in

(c) Elevation height = 22.6 in

(d) Elevation height = 70.0 in

Figure 23. Sludge weight percentage contours at the horizontal planes of four different elevation levels for the four-pump baseline configurations with 70 inch tank liquid level

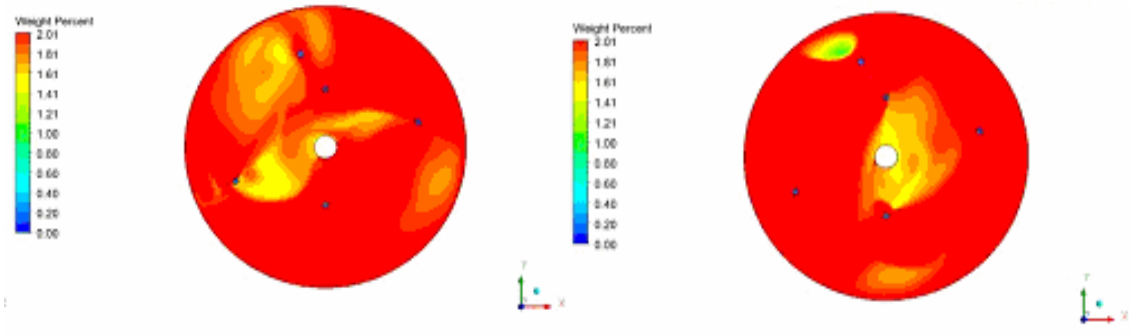

(Four pump operations) (Three pump operations)

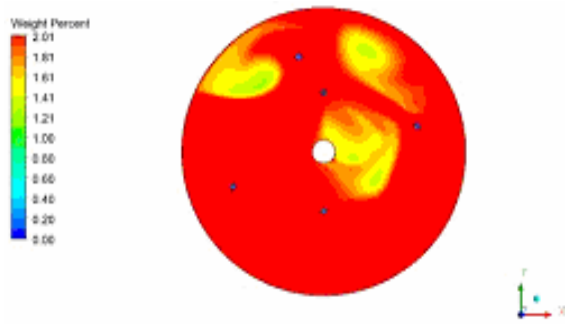

(Two pump operations)

Figure 24. KTPB weight percentage contours at the horizontal planes of transfer pump inlet elevation for various numbers of pumps running with the baseline pump orientations under 70 inch tank liquid level

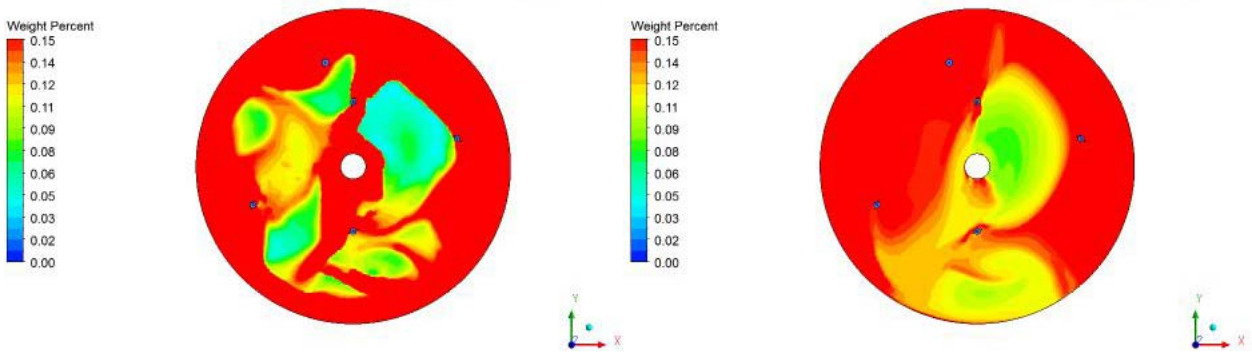

(a) Elevation height = 0.2 in

(b) Elevation height = 9.0 in

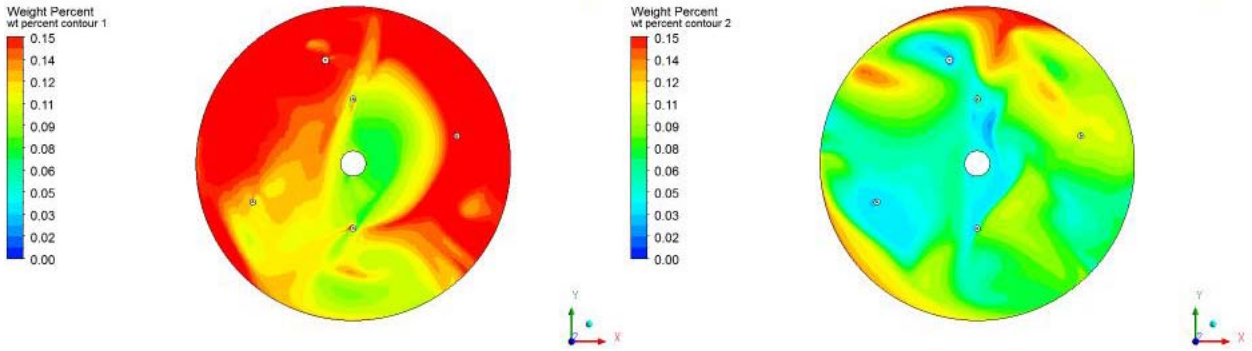

(c) Elevation height = 22.6 in

(d) Elevation height = 70.0 in

Figure 25. MST weight percentage contours at the horizontal planes of four different elevation levels for the two-pump baseline configurations with 70 inch tank liquid level

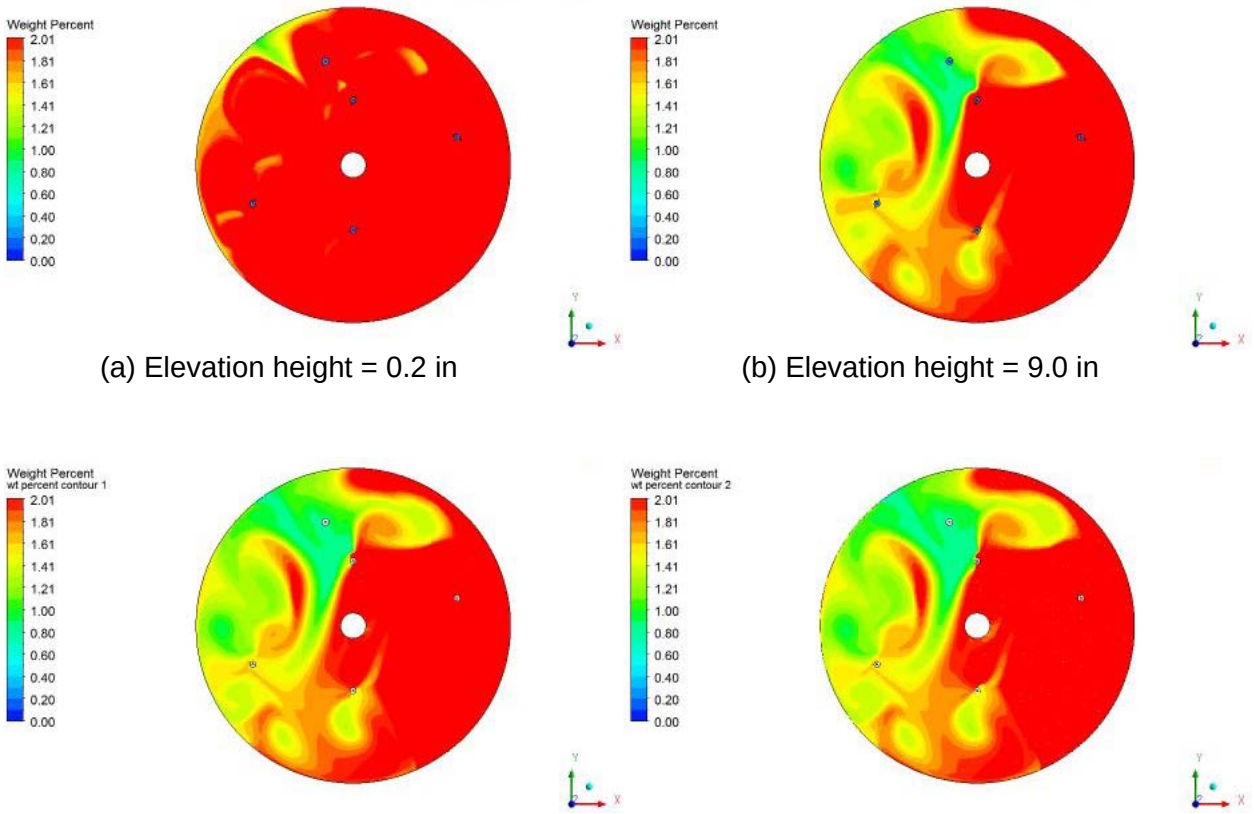

(a) Elevation height = 0.2 in

(b) Elevation height = 9.0 in

(c) Elevation height = 22.6 in

(d) Elevation height = 29.0 in

Figure 26. KTPB weight percentage contours at the horizontal planes of four different elevation levels for the four-pump baseline configurations with 29 inch tank liquid level

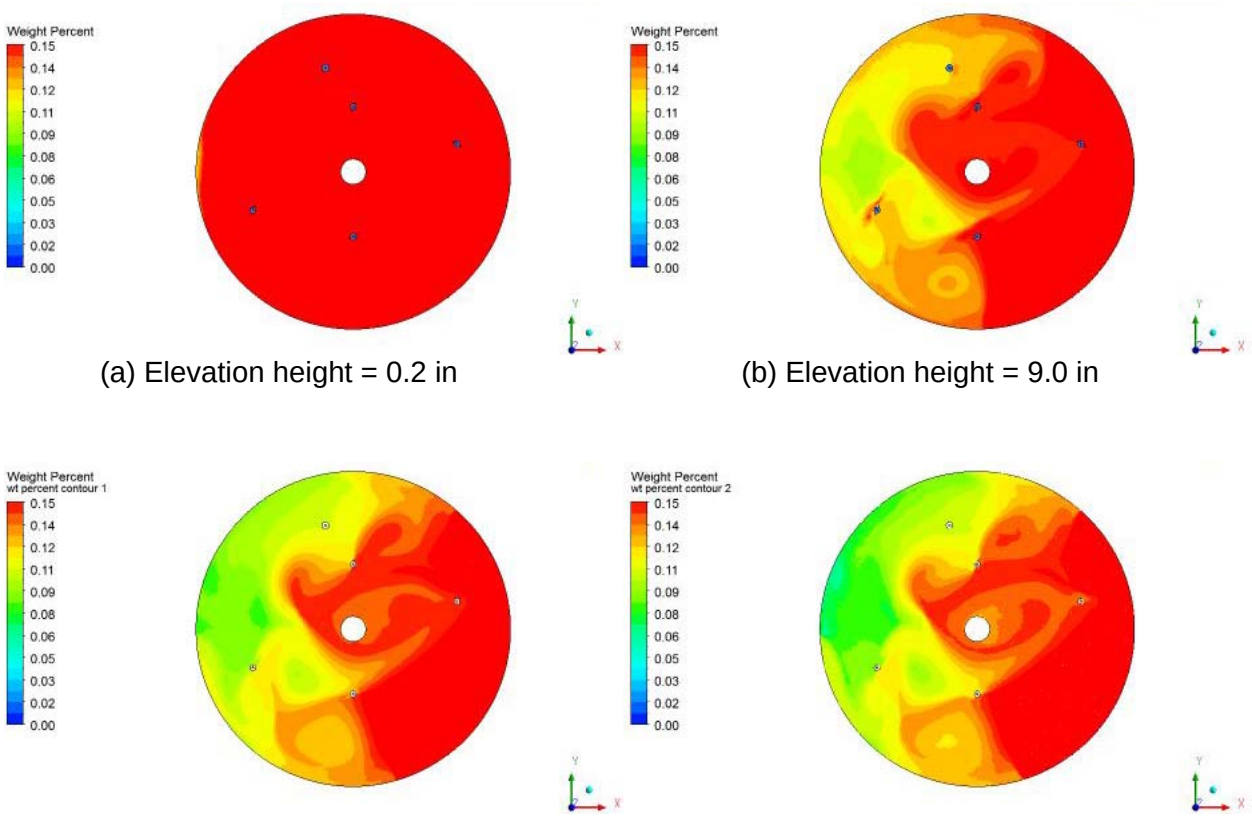

(a) Elevation height = 0.2 in

(b) Elevation height = 9.0 in

(c) Elevation height = 22.6 in

(d) Elevation height = 29.0 in

Figure 27. MST weight percentage contours at the horizontal planes of four different elevation levels for the four-pump baseline configurations with 29 inch tank liquid level

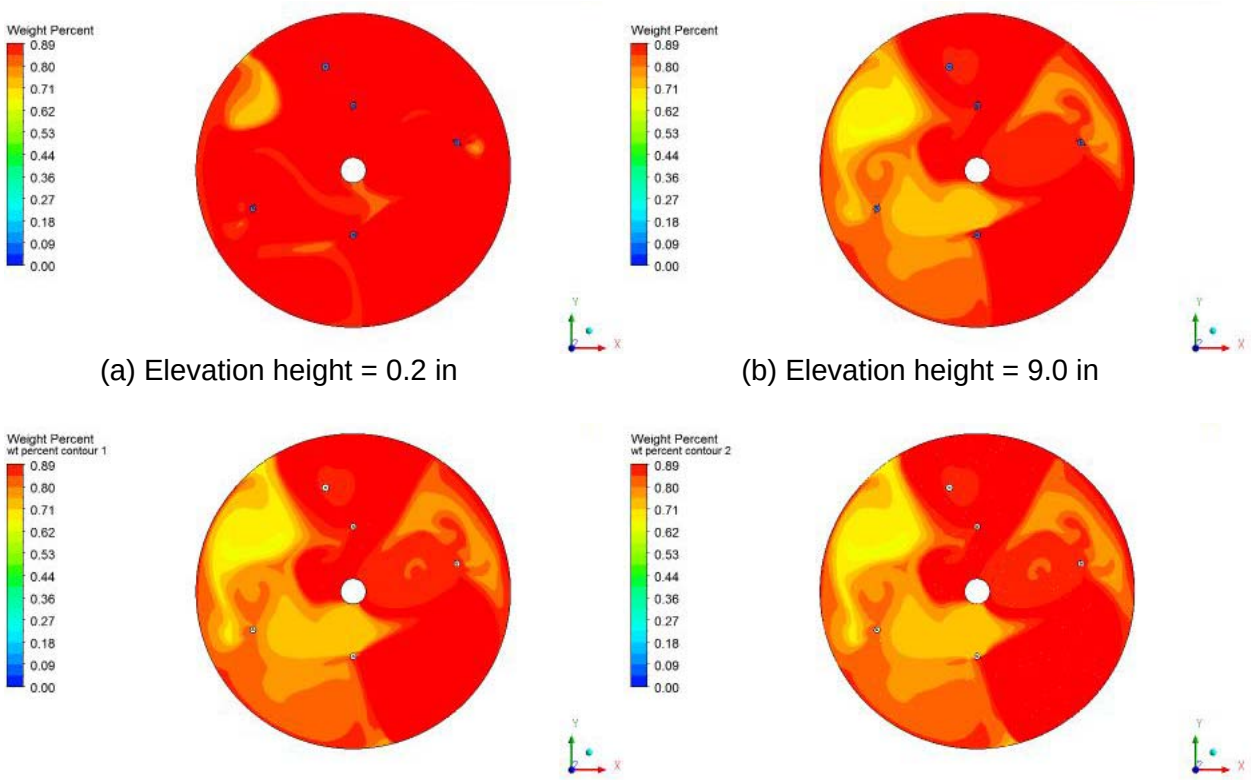

(a) Elevation height = 0.2 in

(b) Elevation height = 9.0 in

(c) Elevation height = 22.6 in

(d) Elevation height = 29.0 in

Figure 28. Sludge weight percentage contours at the horizontal planes of four different elevation levels for the four-pump baseline configurations with 29 inch tank liquid level

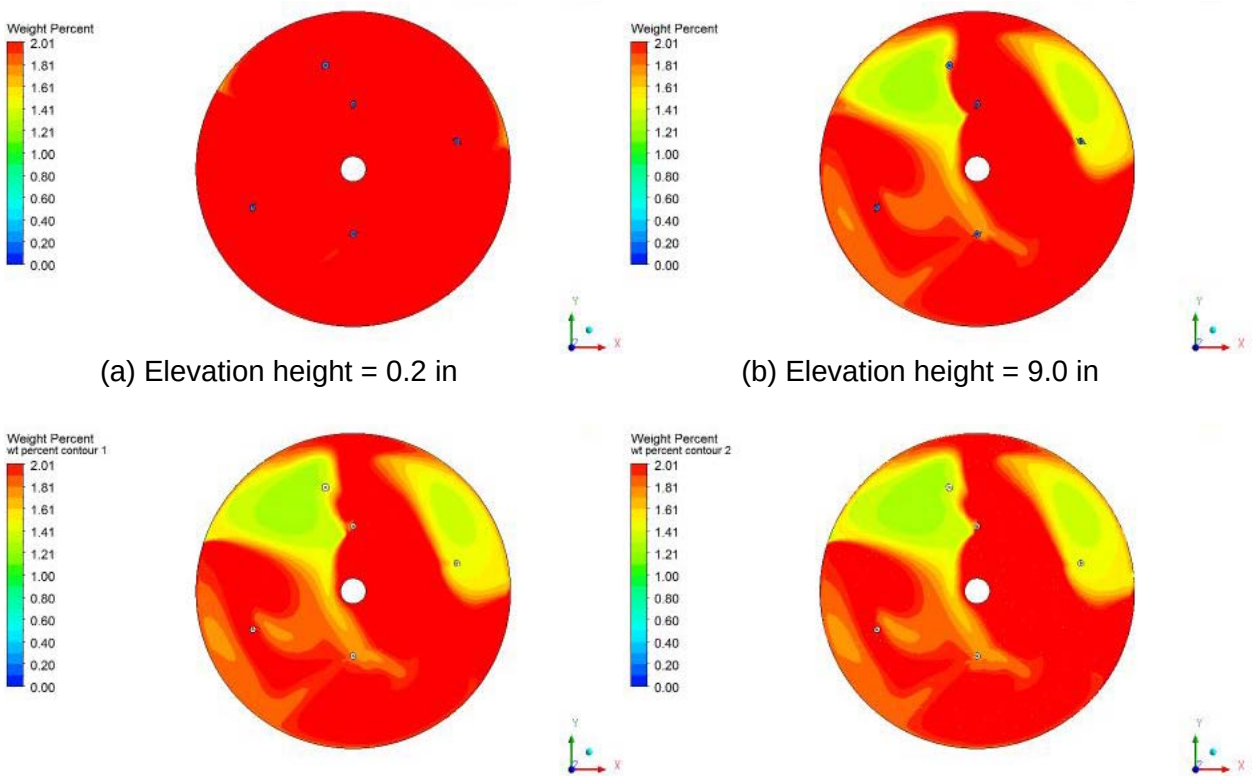

(a) Elevation height = 0.2 in

(b) Elevation height = 9.0 in

(c) Elevation height = 22.6 in

(d) Elevation height = 29.0 in

Figure 29. KTPB weight percentage contours at the horizontal planes of four different elevation levels for the two-pump baseline configurations with 29 inch tank liquid level

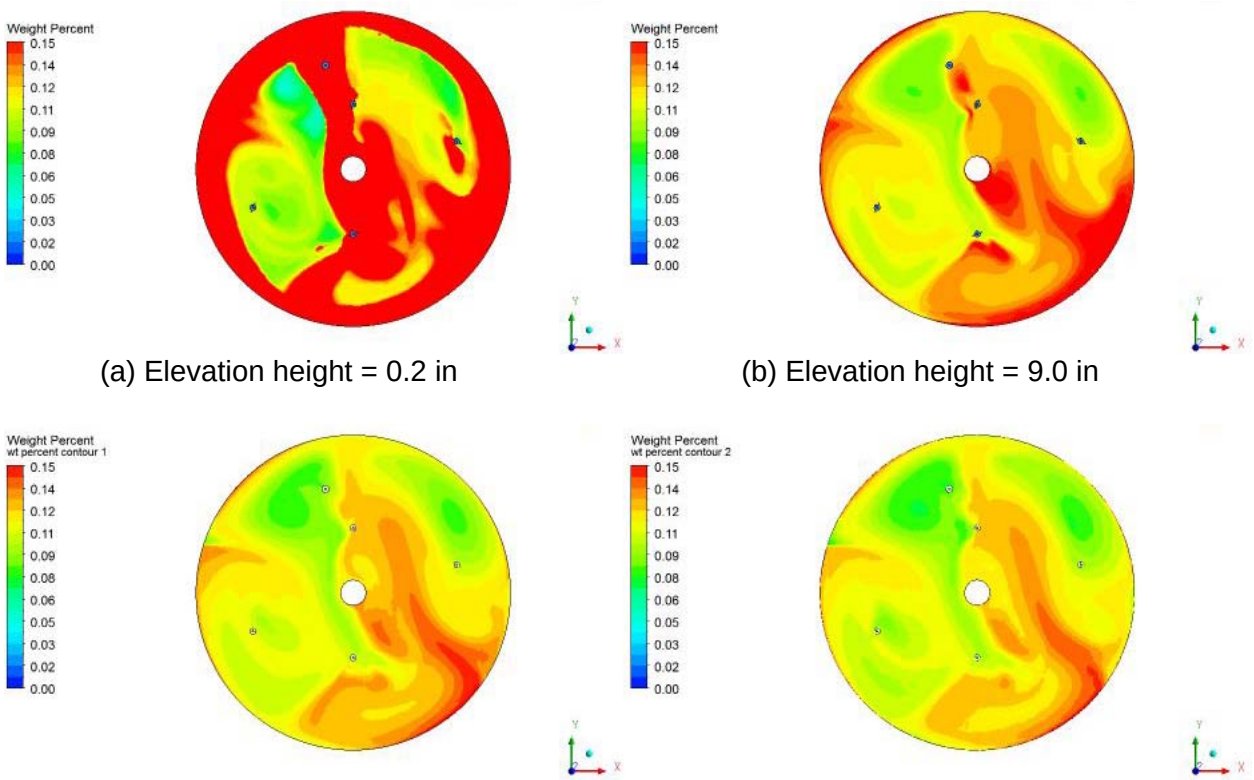

(a) Elevation height = 0.2 in

(b) Elevation height = 9.0 in

(c) Elevation height = 22.6 in

(d) Elevation height = 29.0 in

Figure 30. MST weight percentage contours at the horizontal planes of four different elevation levels for the two-pump baseline configurations with 29 inch tank liquid level

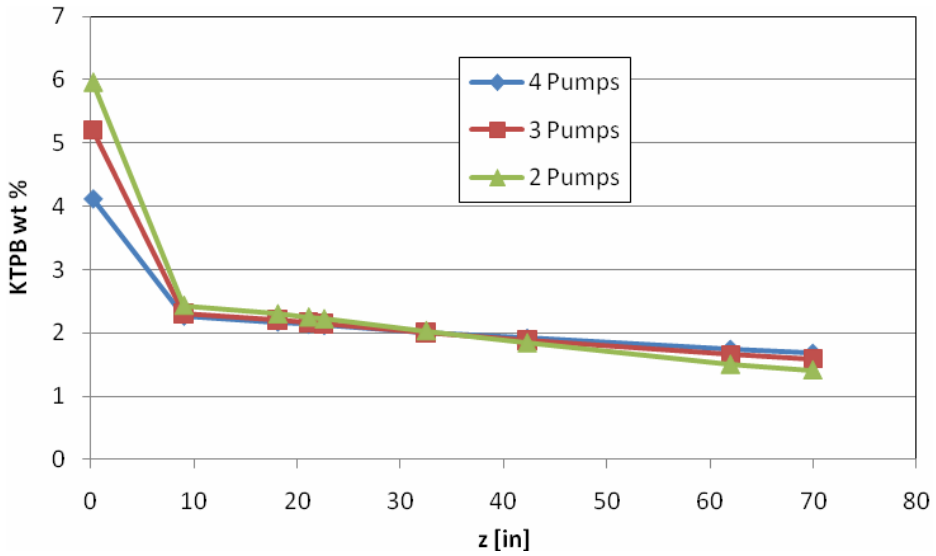

Figure 31. Cross-sectional area-averaged KTPB concentrations for different pump operation conditions in the 70 inch tank liquid level

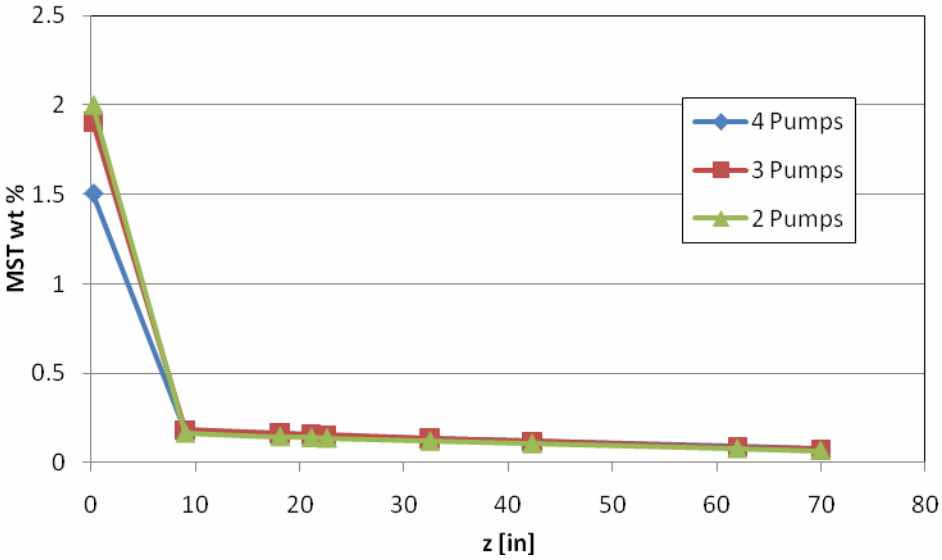

Figure 32. Cross-sectional area-averaged MST concentrations for different pump operation conditions in the 70 inch tank liquid level

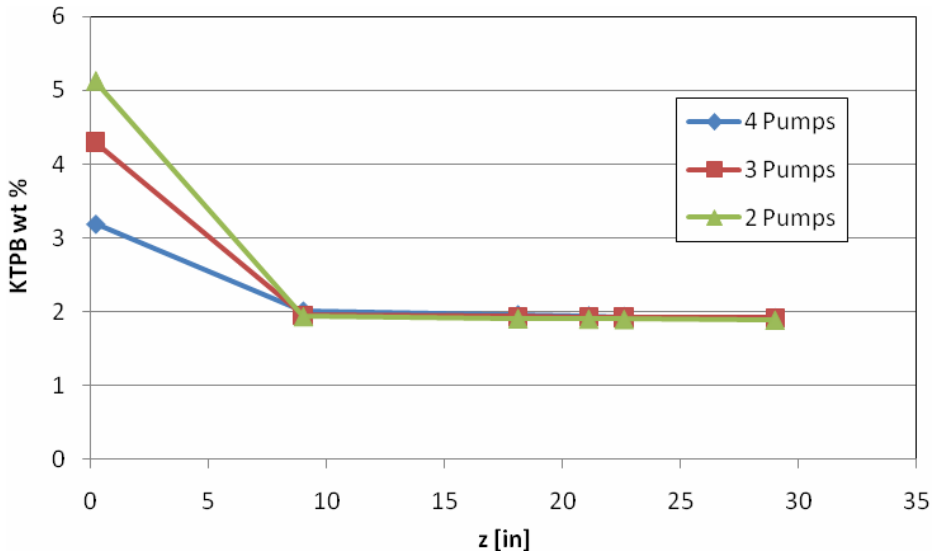

Figure 33. Cross-sectional area-averaged KTPB concentrations for different pump operation conditions in the 29 inch tank liquid level

Table 8. Cross-sectional area-averaged insoluble solid weight percentage for the 70 inches deep tank

	70 inches													
	4 Pump					3 Pump					2 Pump			
	Baseline				90° *	Baseline				90° *	Baseline			
Z [in]	KTPB	MST	Sludge	**Total**	KTPB	KTPB	MST	Sludge	**Total**	KTPB	KTPB	MST	Sludge	**Total**
0.2	4.12	1.51	1.37	**7.00**	3.85	5.21	1.90	1.73	**8.85**	9.46	5.97	2.00	1.99	**9.96**
9	2.27	0.18	0.97	**3.42**	2.18	2.31	0.18	0.99	**3.48**	4.97	2.43	0.16	1.04	**3.64**
18.1	2.17	0.16	0.95	**3.28**	2.11	2.20	0.16	0.96	**3.32**	2.57	2.30	0.15	1.00	**3.45**
21.1	2.14	0.16	0.94	**3.23**	2.08	2.16	0.16	0.95	**3.27**	2.07	2.25	0.14	0.99	**3.37**
22.6	2.12	0.15	0.93	**3.20**	2.07	2.14	0.15	0.94	**3.24**	1.87	2.22	0.14	0.98	**3.33**
32.5	2.01	0.14	0.90	**3.05**	2.00	2.01	0.14	0.90	**3.04**	1.02	2.04	0.12	0.91	**3.06**
42.3	1.92	0.12	0.87	**2.90**	1.94	1.88	0.12	0.85	**2.85**	0.66	1.84	0.11	0.83	**2.78**
62	1.74	0.09	0.80	**2.64**	1.83	1.66	0.09	0.76	**2.51**	0.37	1.50	0.08	0.69	**2.27**
70	1.68	0.08	0.78	**2.54**	1.78	1.59	0.08	0.74	**2.41**	0.32	1.41	0.07	0.66	**2.14**

Note:*Indexed pump orientations rotated by 90° with respect to the baseline orientations corresponding to Case 3 as shown in fig. 9

Table 9. Cross-sectional area-averaged insoluble solid weight percentage for the 29 inches deep tank

	29 inches											
	4 Pump Baseline				3 Pump Baseline				2 Pump Baseline			
Z [in]	KTPB	MST	Sludge	**Total**	KTPB	MST	Sludge	**Total**	KTPB	MST	Sludge	**Total**
0.2	3.19	0.65	1.04	**4.88**	4.30	0.88	1.40	**6.58**	5.13	0.68	1.67	**7.48**
9	2.01	0.14	0.89	**3.04**	1.95	0.14	0.87	**2.96**	1.94	0.12	0.86	**2.92**
18.1	1.96	0.14	0.88	**2.97**	1.94	0.13	0.87	**2.95**	1.92	0.11	0.87	**2.90**
21.1	1.94	0.13	0.88	**2.96**	1.93	0.13	0.88	**2.94**	1.91	0.11	0.87	**2.89**
22.6	1.93	0.13	0.88	**2.95**	1.93	0.13	0.88	**2.94**	1.90	0.11	0.87	**2.89**
29	1.91	0.13	0.88	**2.92**	1.92	0.13	0.88	**2.93**	1.89	0.11	0.87	**2.87**

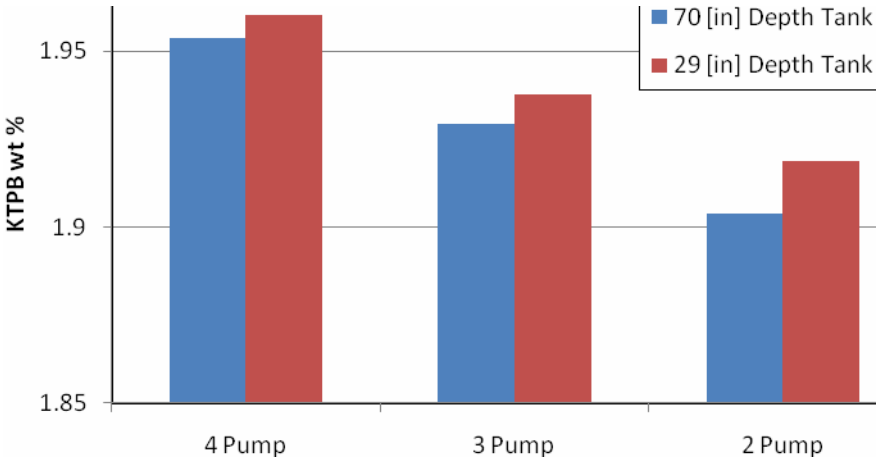

Figure 34. Comparison of the KTPB concentrations averaged by the waste region above the transfer pump inlet plane for different pump operation conditions with two different tank levels (Overall averaged KTPB concentration = 2.01 wt%)

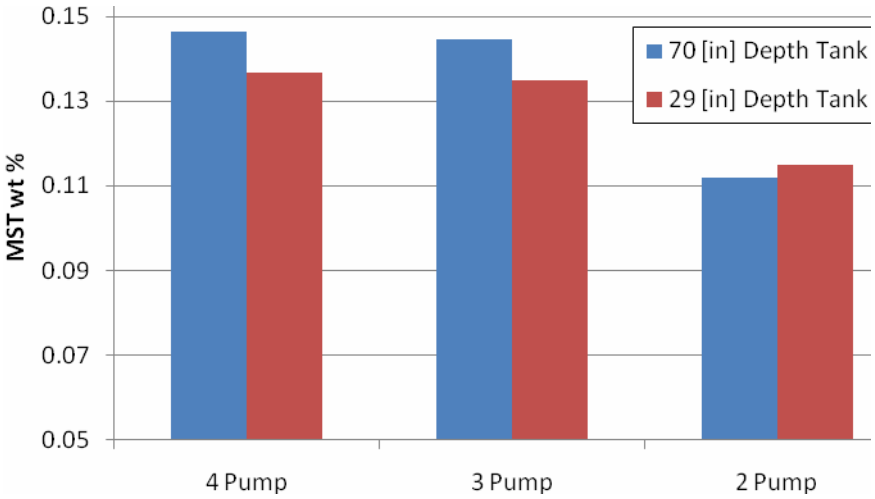

Figure 35. Comparison of the MST concentrations averaged by the waste region above the transfer pump inlet plane for different pump operation conditions with two different tank levels (Overall averaged MST concentration = 0.15 wt%)

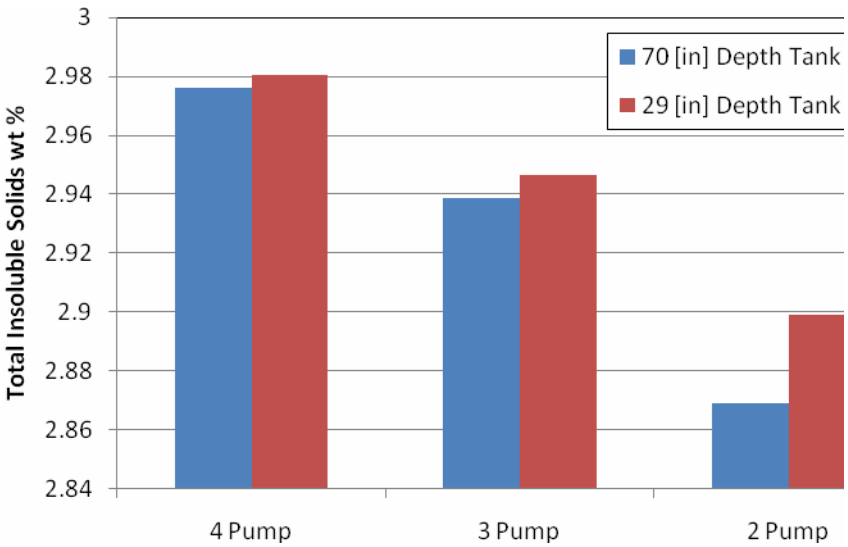

Figure 36. Comparison of the total insoluble solid concentrations averaged by the waste region above the transfer pump inlet plane for different pump operation conditions with two different tank levels (Overall insoluble solid concentration = 3.05 wt%)

5.0 CONCLUSIONS AND SUMMARY

A Tank 48 simulation model with a maximum of four operating slurry pumps has been developed to estimate flow patterns for efficient solid mixing. The modeling calculations were performed by using two approaches. As a primary approach, a single-phase CFD model was developed to evaluate the flow patterns and qualitative mixing behaviors for a range of different operating conditions since the model was previously benchmarked against the test results [Lee et al., 2008]. As a secondary approach, a two-phase CFD model was developed to estimate solid concentrations in a quantitative way by solving the Eulerian governing equations for the continuous fluid and insoluble solid phases over the entire tank domain. The calculation results for the two approaches were qualitatively compared for the same modeling conditions. The two-phase results should be considered as scoping calculations since the model was not validated against the test results.

A series of sensitivity calculations for different numbers of operating pumps and operating conditions have been performed to provide operational guidance for solids suspension and mixing in Tank 48. In the analysis, the pumps were assumed to be stationary. Major solid obstructions such as the pump housing, the pump columns, and the 82 inch central support column were included. Steady state analyses coupled with a two-equation turbulence model for the uncoiled tank were performed with the FLUENT™ and CFX™ codes. All analyses were based on three-dimensional results. Recommended operational guidance was developed assuming that local fluid velocity can be used as a measure of solids suspension and spatial mixing under a single-phase tank model. For quantitative analysis, a two-phase fluid-solid model was developed for the same modeling conditions as the single-phase model.

The main conclusions drawn from the Tank 48 modeling and calculations are as follows:

- The recent results [Lee et al., 2008; Lee and Armstrong, 2011] show that it takes about one hour to suspend the tank solids adequately at the transfer pump suction with four slurry pump operations in Tank 48.
- Estimations of minimum suspension velocity and particle settling rate were made for establishment of a flow velocity criterion required for solids suspension and for determination of settling time after stoppage of slurry pump operation.
- The two baseline models of the single-phase and two-phase simulations were developed with four pumps operating to evaluate flow circulation patterns and solid concentrations for the solid mixing operations of Tank 48. The flow pattern results for the single-phase model are qualitatively consistent with those of the two-phase model.
- The calculation results show that the flow patterns driven by four pump operation satisfy the solid suspension requirement, and the average solid concentration at the plane of the transfer pump inlet is about 12% higher than the tank average concentrations for the 70 inch tank level and about the same as the tank average value for the 29 inch liquid level.
- The flow pattern results show that when more than one jet are aiming at the same position of the mixing tank domain, inefficient flow patterns are provided due to the highly localized momentum dissipation, resulting in inactive suspension zone. Thus, after completion of the indexed solids suspension, pump rotations are recommended to avoid producing the non-uniform flow patterns.
- The modeling results show that when one of the four pumps is not operated, the flow patterns satisfy the minimum suspension velocity criterion. However, the solid concentration near the tank bottom is increased by about 30% as shown in Figs 31

to 33, although the average solid concentrations near the transfer pump inlet have about the same value of the four-pump baseline results.

- The modeling results show that although the two-pump case satisfies the local velocity requirement to suspend the sludge particles as shown in Fig. 19, it provides marginal mixing results for the heavier or larger insoluble materials such as MST and KTPB solids.
- The sensitivity results show that when more slurry pumps are operated for the loosely-packed solids layer settled down on the tank floor, the wall boundary region has more steep concentration gradient with respect to the layer thickness, but the upper half region of the tank liquid has the solid concentrations closer to the tank-average value. For more pumps operating, the solid mixing efficiency is improved significantly in terms of local solid concentration as expected.
- The sensitivity results show that the pump orientation has a large impact on the flow patterns.
- The two-phase modeling results indicate that when less pumps are operated for a given tank level, the spatial concentrations for the heavier or larger solids become less uniform, especially, at the bottom and top planes.
- It is noted that when tank liquid level is reduced from the highest level of 70 inches to the minimum level of 29 inches for a given number of operating pumps, the solid concentrations become more uniform over the tank fluid domain since the ratio of the pump power to the mixing volume becomes larger. These results are consistent with the literature results.

Based on the initial scoping results of the CFD modeling study, the responses to the technical request items listed in TTR [Jacobs, 2010] are summarized as follows:

Item (a): Minimum three pump runs are required for the adequate mixing of the tank solids at the elevation level of the transfer pump suction although two pump operations have marginal results for the MST and KTPB solids. Based on the recent results [Lee et al., 2008; Lee and Armstrong, 2011], about one-hour operation is needed to suspend the tank solids adequately at the transfer pump suction with slurry pump operations in Tank 48.

Item (b): When the tank solids are adequately suspended at the beginning of the slurry pump outage, a couple of hours will be needed to settle down the solids on the tank floor after stoppage of slurry pump operation. This is conservatively estimated by the settling rate under the frozen fluid motion.

Item (c): The volume-averaged weight percentages of each insoluble particles in the volume above the transferred pump inlet are summarized in Table 10. Neglecting any temporal effects of particle sedimentation during the FBSR transfer process, the solid concentrations of particles averaged by the tank content volume will be removed from the tank as shown in Table 9.

Item (d): The unsuspended particles during the mixing process are accumulated on the tank floor within a 0.2 inch thick layer as shown in Table 11.

Item (e): The flow pattern results show that when more than one jet are aiming at the same position of the mixing tank domain, inefficient flow patterns are generated due to the highly localized momentum dissipation. Thus, after completion of the indexed solids suspension, pump rotations are recommended to prevent the non-uniform flow patterns. The initial

scoping steady-state results show that about 95 wt % of the particles will be suspended under more than 2 pumps operation condition. Two-pump operation is not recommended for the FBSR process.

Table 10. Comparison of solid concentrations during the transfer process

# of pumps	Tank level (inches)	Total wt %	Solids*			Total
			KTPB Avg. wt%: 2.01	MST Avg. wt%: 0.15	Slurry Avg. wt%: 0.89	Avg. wt%: 3.05
4	70	3.05	1.9538	0.1467	0.8759	2.9764
4	29	3.05	1.9600	0.1491	0.8839	2.9930
3	70	3.05	1.9291	0.1493	0.8542	2.9326
3	29	3.05	1.9377	0.1495	0.8580	2.9451
2	70	3.05	1.9037	0.1486	0.8755	2.9278

Note:*Volume-averaged solid concentrations for the tank content volume above the transfer pump inlet (9” elevation above the tank floor)

Table 11. All particle concentrations for the baseline operating scenarios considered for the two-phase modeling approach

# of operating pumps	Tank liquid level (inches)	Insoluble solids conc. (KTPB, MST, and sludge) (wt %)		
		Near transfer pump inlet (9 inches from tank floor)	Tank floor (0.2 inch thick layer on tank floor)	Average concentration
4	70	4.58	16.22	3.05
4	29	2.04	9.00	3.05
3	70	4.85	25.44	3.05
3	29	1.94	17.42	3.05
2	70	5.64	32.31	3.05
2	29	3.07	18.52	3.05

Item (f): When solid contents are changed from the initial concentrations of 3.05 wt% to 0 wt% at the end of the FBSR processing, solid concentrations in the fluid will become slowly decreased during the FBSR process since the solids settled on the tank floor will become heavier and larger after each of the transfer operations. However, the current scoping model did not consider a transient settling behavior during the solids suspension. The modeling and simulations combined with a series of different pump orientations are required to evaluate the solid contents in the tank fluid at each of the transfer processes in a quantitative way.

6.0 REFERENCES

1. J. R. Jacobs, "Technical Task Request for Tank 48 Mixing Study", X-TTR-H-00012, August 2010.
2. S. Y. Lee and R. A. Dimenna, "Task Plan for tank 48 Mixing Study", SRNL-TR-2010-00273, September 2010.
3. S. Y. Lee, R. A. Dimenna, R. A. Leishear, D. B. Stefanko, "Analysis of Turbulent Mixing Jets in a Large Scale Tank", ASME *Journal of Fluids Engineering*, Volume 130, Number 1, pp. 011104, 2008.
4. S. Cutts, "Tank 48 Project Design Basis Document," DB-21-001, Rev B, March 2010.
5. S. C. Shah, "Tank 48 Feed Chemical and Radionuclide Compositions," X-CLC-H-00646, Rev 3, July 2010.
6. BPF216146, "Hydraulic Test Data Sheet," (BPF216146 30 0) 1C023
7. T. C. Baughman, "Fluidized bed Steam Reformer (FBSR) Process Rheology Technical report", M-TRT-H-00069, Rev. 0, March 2010.
8. Technical Communications with M. R. Poirier, January 12, 2011, and WSRC-TR-97-0360, Rev. 0, page 13, 1997.
9. M. R. Poirier, et al, "Particle Size of Simulated SRS Sludge, Actual SRS Sludge, and Monosodium Titanate," WSRC-TR-2003-00221, May 2003.
10. J. L. Thomas, "Tank 48 Best Estimate Chemical Characterization", CBU-PIT-2005-00066, May 2006.
11. D. T. Hobbs, "RF-120: MST Density Difference", SRNL-CST-2007-00007, January 19, 2007.
12. Drawing#: W803562, Rev 32, "T48 Chemical Feed and Service Piping Arrangement Plan," September 1996.
13. Drawing#: W809829, Rev 12, "Tank 48 Structural Steel," February 2004.
14. Drawing#: W801762, Rev 16, "Equipment and Piping Arrangement Plan," March 2005.
15. S. Y. Lee and B. W. Armstrong, "SDI CFD Modeling Analysis", SRNL-STI-2011-00025, April 2011.
16. Abramovich, G. N., "*The Theory of Turbulent Jets*", The MIT Press, Cambridge, MA, 1963.
17. S. Y. Lee, R. A. Dimenna, R. A. Leishear, and D. B. Stefanko, "Mixing in Large Scale Tanks Part I; Flow Modeling of Turbulent Mixing Jets", HT-FED2004-5622, 2004 ASME Heat Transfer / Fluids Engineering Summer Conference, Charlotte, N. C., July 11-15, 2004.
18. E. Hansen and G. Daniel, "Summary of SRNL Tank 48 Sample Data", SRNL-PSE-2008-000341, Rev 0, February 8, 2008.
19. S. Hyun, "Computer Modeling and Simulation for High-Level Waste Mixing", Project report for SRNL prepared under subcontract number: G-SOW-A-00455, Mercer University, Macon, GA, March 10, 2011.
20. S. Y. Lee and R. A. Dimenna, "Slurry Pump Mixing Effectiveness in Tank 50H", Savannah River national Laboratory, WSRC-STI-2008-00151, February 2008.
21. C. Eckart, "An Analysis of the Stirring and Mixing Processes in Incompressible Fluids", J. Mar. Research, vol. 7, pp. 265 – 275, 1948.
22. D. B. Spalding, "Mixing and Chemical Reaction in Steady Confined Turbulent Flames", 13th International Symposium on Combustion, 649-657, 1971.
23. P. L. Miller, 1991, "Mixing in High Schmidt Number Turbulent Jets", PhD Thesis, California Inst. of Technology.
24. D. R. Oliver, "The Sedimentation of Suspensions of Closely-Sized Spherical Particles", *Chemical Engineering Science*, Vol. 15, pp. 230-242, 1961.

25. W. H. Graf, *Hydraulics of Sediment Transport*, McGraw-Hill Book Company (1971).
26. *FLUENT*, Fluent, Inc., 2003
27. G. B. Tatterson, *Fluid Mixing and Gas Dispersion in Agitated Tanks*, McGraw-Hill, Inc., 1991.
28. H. B. Fischer, "Longitudinal Dispersion and Turbulent Mixing in Open-Channel Flow", Annual Review of Fluid Mechanics, Vol. 5, pp. 59-78, 1973.
29. J. Baldyga and J. R. Bourne, "A Fluid Mechanical Approach To Turbulent Mixing and Chemical Reaction, Part III Computational and Experimental Results for the New Micromixing Model", CHEM. Eng. Commun., Vol. 28, pp. 259-281, 1984.
30. J. J. Perona, T. D. Hylton, E. L. Youngblood, and R. L. Cummins, "Jet Mixing of Liquids in Long Horizontal Cylindrical Tanks", Ind. Eng. Res., Vol. 37, pp. 1478-1482, 1998.
31. R. K. Grenville and J. N. Tilton, "A New Theory Improves the Correlation of Blend Time Data from Turbulent Jet Mixed Vessels", Trans. Inst. of Chem. Eng., Vol. 74, Part A., pp. 390-396, April 1996.
32. R. K. Grenville and J. N. Tilton, "Turbulent Flow or Flow as a Predictor of Blend Time in Turbulent Jet Mixed Vessels", Proceedings of 9th European Conf. on Mixing, pp. 67-74, 1997.
33. M. Simon and C. Fonade, "Experimental Study of Mixing Performances Using Steady and Unsteady Jets", The Canadian J. of Chem. Eng., Vol. 71, 1993.
34. Forstall, W., Jr. and Shapiro, A. H., "Momentum and Mass Transfer in Coaxial Gas Jets", *Journal of Applied Mechanics*, pp. 399-408, December 1950.
35. Ricou, F. P. and Spalding, D. B., "Measurements of Entrainment by Axisymmetrical Turbulent Jets", *Journal of Fluid Mechanics*, Vol. 11, pp. 21-32, 1961
36. Fossett, H. and Prosser, L. E., "The Application of Free Jets to the Mixing of Fluids in Bulk", J. of Inst. of Mechanical Engineers, Vol. 160, No. 2, pp. 224-232, 1949.
37. E. A. Fox and V. E. Gex, "Single-phase Blending of Liquids", A.I.Ch.E. Jorunal, Vo. 2, No. 4, pp. 539-544, December 1956.
38. Okita, N. and Oyama, Y., "Mixing Characteristics in Jet Mixing", Chemical Engineering, The Society of Chemical Engineers, Japan, Vol. 1, No. 1, pp. 92-101, 1963.
39. Lane, A. G. C. and Rice, P., "An Investigation of Liquid Jet Mixing Employing an Inclined Side Entry Jet", Inst. of Chemical Engineers, Vol. 60, pp. 171-176, 1982.
40. W. M. Kays and M. E. Crawford, *Convective Heat and Mass Transfer*, Second Edition, McGraw-Hill Book Company, New York, 1980.
41. Kiser, K. M., "Material and Momentum Transport in Axisymmetric Turbulent Jets of Water", *A.I.Ch.E. Journal*, Vol. 9, No. 3, pp. 386-390, 1963.
42. Post, S., 1998, "A Computational and Experimental Study of Near-Field Entrainment in Steady Gas Jets," MSME thesis, Purdue University.
43. Hinze, J. O., *Turbulence, Second Edition*, McGraw-Hill, New York, p. 72, 1975.
44. Tennekes, H. and Lumley, J. L., *A First Course in Turbulence*, The MIT Press, Cambridge, 1972.
45. Leishear, R. A., Poirier, M. R., and Fowley, M. D., "SDI Blend and Feed Blending Pump Design Phase 1 (U)", Savannah River National Laboratory, SRNL-STI-2010-00054, March 2010.